Enclosure 3

KP-TR-022-NP "Hermes 2 Postulated Event Methodology" Revision 1

(Non-Proprietary)

KP-TR-022-NP

Kairos Power LLC
707 W. Tower Ave
Suite A
Alameda, CA 94501

Hermes 2 Postulated Event Methodology

Technical Report

Revision No. 1
Document Date: May 2024

Non-Proprietary

COPYRIGHT Notice

This document is the property of Kairos Power LLC (Kairos Power) and was prepared in support of the development of the KP Fluoride Salt-Cooled High Temperature Reactor (KP-FHR) design. Other than by the NRC and its contractors as part of regulatory reviews of the KP-FHR design, the content herein may not be reproduced, disclosed, or used, without prior written approval of Kairos Power.

Rev	Description of Change	Date
0	Initial Issuance	June 2023
1	Added reference to intermediate coolant pump in Section 3.2.2.7. Added reference to radioactive release from subsystem or component in Table 3-2	May 2024

© 2024 Kairos Power LLC

Executive Summary

This report describes the postulated events and the methodology that, when used to evaluate events within the design basis, ensures there are sufficient design features available to mitigate their effects and keep the potential consequences bounded by the maximum hypothetical accident (MHA).

Figures of merit are derived for the postulated events to provide surrogate metrics which demonstrate that the resulting dose is bounded by the dose consequences of the MHA analysis. Acceptance criteria for these figures of merit represent design limits that ensure the MHA is bounding.

The evaluation models used to analyze the postulated events are described as well as the associated verification and validation plans. Sample postulated event analyses are provided in appendix as an illustration of the methods described in this report.

The MHA is summarized in this report only to provide context for the derivation of figures of merit for postulated events that when evaluated ensure that the dose is bounded by an MHA with acceptable dose consequences.

© 2024 Kairos Power LLC

Table of Contents

1 Introduction 8
1.1 Design Features 8
1.1.1 Design Background 8
1.1.2 Key Design Features of the KP-FHR 8
1.2 Regulatory Background 9
2 Maximum Hypothetical Accident Summary 11
2.1 Maximum Hypothetical Accident Narrative 11
2.2 Maximum Hypothetical Accident Temperature Curve 11
2.3 Conservative Release Models 11
2.4 Results 17
3 Capability of Evaluation Models 18
3.1 Overview of Evaluation Models for Postulated Events 18
3.2 Evaluation Model Applicability 18
3.2.1 Postulated Event Categories and Duration of Evaluation 18
3.2.2 Postulated Events 18
3.2.3 Evaluation Models Used to Analyze Postulated Events 28
3.3 Phenomena Identification and Ranking Tables 28
3.4 Figures of Merit 29
3.4.1 Dose Acceptance Criteria 29
3.4.2 Postulated Event Figures of Merit 29
4 Evaluation Models 34
4.1 Systems Analysis 34
4.1.1 KP-SAM Code Description 34
4.1.2 KP-SAM Verification and Validation Plan 37
4.1.3 Plant KP-SAM Model 37
4.2 Fuel Performance 38
4.3 Neutronics 40
4.4 Structural Analysis 40
4.5 Event-Specific Methods 40
4.5.1 Salt Spills 40
4.5.2 Insertion of Excess Reactivity 44
4.5.3 Loss of Forced Circulation 45
4.5.4 Pebble Handling and Storage System Malfunction 47
5 Conclusions 53
6 References 54
APPENDIX A.Sample Transient Results 69

© 2024 Kairos Power LLC

Tables and Figures

Table 2-1: Prescriptive Maximum Hypothetical Accident Temperatures 56
Table 3-1: Analyzed Postulated Events and Applied Evaluation Models 57
Table 3-2: Derived Figures of Merit and Acceptance Criteria for Postulated Events 58
Table 4-1: KP-SAM Models and Field Equations 60
Table 4-2: Sample KP-SAM Input Components by Nodal Type 61
Table 4-3: KP-FHR TRISO fuel specification for as-manufactured contamination and defect fractions 62
Table 4-4: Input Parameters Considered for Postulated Events 63
Figure 1-1: Elements of Evaluation Model Development and Assessment Process 65
Figure 2-1: Prescriptive MHA Temperatures 66
Figure 4-1: SAM Code Structure 67
Figure 4-2: KP-SAM Sample Nodal Diagram 68
Table A1-1: Initial conditions for Insertion of Excess Reactivity Assumed Bounding Event 71
Table A1-2: 95% Confidence Level Upper Limit on In-Service Failure Fractions for Normal Operation and Reactivity Insertion Postulated Event 72
Table A1-3: Compromised Fractions for Normal Operation and Reactivity Insertion Postulated Event 73
Figure A1-1: Reactivity Insertion and Reactivity Feedback After Full Rod Withdrawal 74
Figure A1-2: Figures of Merit During and After Reactivity Insertion 75
Figure A2-1: Normalized Reactor Power vs Instantaneous Average Fuel and Cooling Temperature Drop 77
Table A3-1: Key Input Parameters 80
Table A3-2: Properties of Spilled Flibe and Building Air 81
Table A3-3: Calculated Values for the Salt Spill Event 82
Table A4-1: Initial Conditions for Loss of Forced Circulation Overheating Assumed Bounding Event 85
Table A4-2: Initial Conditions for Loss of Forced Circulation Overcooling Assumed Bounding Event 86
Table A4-3: Irradiation Conditions for Simulated Normal Operation 87
Table A4-4: Inputs for Loss of Forced Circulation Postulated Events 88
Table A4-5: 95% Confidence Level Upper Limits on In-Service Failure Fractions for Normal Operation and Loss of Forced Circulation Postulated Events 89
Table A4-6: Compromised Fractions for Normal Operation and Loss of Forced Circulation Postulated Event 90
Figure A4-1: Figures of Merit – Overheating 91
Figure A4-2: Figures of Merit – Overcooling 92
Table A5-1: Key Input Parameters for Pebble Handling and Storage System Malfunction Event 96
Table A5-2: Total Activities and Activities for Selected Elements in Graphite Matrix in Pebbles with Highest Burnup 97
Figure A5-1: Graphite Oxidation Rate 98
Figure A5-2: Mass Loss of Graphite Matrix and Release Fraction of MAR 99
Figure A5-3: Temperature of the Outer Surface of the Pebble 100

© 2024 Kairos Power LLC

List of Acronyms

C/HM	carbon-to-heavy-metal atom ratio
DHRS	decay heat removal system
EAB	exclusion area boundary
EMDAP	evaluation model development and assessment process
HRR	heat rejection radiator
LPZ	low population zone
LWR	light water reactors
MAR	radioactive material at risk for release
MHA	maximum hypothetical accident
MHTGR	Modular High Temperature Gas-Cooled Reactor
MOOSE	Multiphysics Object Oriented Simulation Environment
PHSS	pebble handling and storage system
IHX	intermediate heat exchanger
PIRT	Phenomena identification and ranking table
PSP	primary salt pump
RCSS	reactivity control and shutdown system
RF	release fraction
RG	regulatory guide
SSCs	structures, systems, and components
TRISO	tri-structural isotropic

© 2024 Kairos Power LLC

1 INTRODUCTION

This report details the postulated events that must be considered and the transient methodology that, when used to evaluate events within the design basis, ensures there are sufficient design features available to mitigate the effects and keep the potential consequences bounded by the maximum hypothetical accident (MHA). Consistent with the guidance in NUREG 1537, "Guidelines for Preparing and Reviewing Applications for the Licensing of Non-Power Reactors", an MHA is used to demonstrate that the radiological consequences from a bounding event result in acceptable dose levels.

Events within the design basis are referred to as postulated events. All postulated events must be considered to ensure there are sufficient design features available to mitigate the effects and keep the potential consequences bounded by the MHA, consistent with the requirements in 10 CFR 50.34(a).

An MHA is summarized in Section 2 only to provide context for the derivation of figures of merit for postulated events that function as surrogates for dose. The MHA that demonstrates dose compliance for the design is provided in the licensing application. An MHA is an event with hypothetical conditions designed to result in a release of radionuclides from the fuel. The hypothetical fuel release, along with hypothetical conditions that result in the release of other radioactive material at risk for release (MAR) contained in the primary system, results in a reasonably bounding dose at the site boundary. The MHA dose is reasonably bounding because it is based on non-physical conditions that are beyond the design basis. This report details the derivation of figures of merit from the MHA conditions, but the final numbers for the acceptance criteria are based on the MHA presented in the licensing application.

1.1 DESIGN FEATURES

1.1.1 Design Background

This technical report provides transient methods based on a KP-FHR design. Key design features are provided in this section which are considered inherent to the KP-FHR technology. These provide the basis to support the safety review of the transient methodology.

The KP-FHR is a U.S.-developed Generation IV advanced reactor technology. In the last decade, U.S. national laboratories and universities have developed pre-conceptual Fluoride Salt-Cooled High Temperature Reactor (FHR) designs with different fuel geometries, core configurations, heat transport system configurations, power cycles, and power levels. More recently, University of California at Berkeley developed the Mark 1 pebble-bed FHR, incorporating lessons learned from the previous decade of FHR pre-conceptual designs (Reference 1). Kairos Power has built on the foundation laid by Department of Energy-sponsored university Integrated Research Projects to develop the KP-FHR.

Additional design description information for KP-FHR power reactor technology is provided in the "Design Overview of the Kairos Power Fluoride Salt-Cooled, High Temperature Reactor (KP-FHR)" Technical Report (Reference 2).

1.1.2 Key Design Features of the KP-FHR

The KP-FHR is a high temperature reactor with molten fluoride salt coolant operating at near-atmospheric pressure. The fuel in the KP-FHR is based on the Tri-Structural Isotropic (TRISO) high-temperature carbonaceous-matrix coated particle fuel in a pebble fuel element developed for high-temperature gas-cooled reactors. Coatings on the particle fuel provide retention of radionuclides. The reactor coolant is a chemically stable molten fluoride salt mixture, $2{\cdot}^{7}$LiF:BeF2 (Flibe with enrichment of the ^{7}Li isotope) which also provides retention of radionuclides that escape from any fuel defects. A

© 2024 Kairos Power LLC

primary coolant loop circulates the reactor coolant using pumps and transfers the heat to the intermediate coolant via a heat exchanger. The pumped flow intermediate coolant loop utilizes a salt coolant, which is compatible with the reactor coolant, and transfers heat from the reactor coolant to the power generation system through a superheater. The design includes decay heat removal capability for both normal conditions and accident conditions. Passive decay heat removal, along with natural circulation in the reactor vessel, is used to remove decay heat in response to a postulated event. The KP-FHR does not rely on electrical power to achieve and maintain safe shutdown for design basis accidents.

The KP-FHR design relies on a functional containment approach similar to the Modular High Temperature Gas-Cooled Reactor (MHTGR) instead of the typical light water reactor (LWR) low-leakage, pressure retaining containment structure. The KP-FHR functional containment safety design objective is to meet 10 CFR 50.34 (10 CFR 52.79) offsite dose requirements at the plant's exclusion area boundary (EAB) with margin. A functional containment is defined in RG 1.232, “Developing Principal Design Criteria for Non-Light Water Reactors” as a "barrier, or set of barriers taken together, that effectively limit the physical transport and release of radionuclides to the environment across a full range of normal operating conditions, anticipated operational occurrences, and accident conditions.” RG 1.232 includes an example design criterion for the functional containment (MHTGR Criterion 16). As also stated in RG 1.232, the Nuclear Regulatory Commission has reviewed the functional containment concept and found it “generally acceptable,” provided that “appropriate performance requirements and criteria” are developed. The Nuclear Regulatory Commission staff has developed a proposed methodology for establishing functional containment performance criteria for non-LWRs, which is presented in SECY-18-0096, “Functional Containment Performance Criteria for Non-Light-Water-Reactors”. This SECY has been approved by the Commission.

The functional containment approach for the KP-FHR is to control radionuclides primarily at their source within the coated fuel particle under normal operations and accident conditions without requiring active design features or operator actions. The KP-FHR design relies primarily on the multiple barriers within the TRISO fuel particles to ensure that the dose at the site boundary as a consequence of postulated accidents meets regulatory limits. However, in the KP-FHR as opposed to the MHTGR, the molten salt coolant serves as a distinct additional barrier providing retention of radionuclides that escape the fuel particle and fuel pebble barriers. This additional retention is a key feature of the enhanced safety and reduced source term in the KP-FHR.

1.2 REGULATORY BACKGROUND

Applicants for a non-power reactor construction permit must prepare a preliminary safety analysis report in accordance with the regulations in 10 CFR 50.34(a)(1)(i) and 10 CFR 50.34(a)(2) through 10 CFR 50.34(a)(8). The dose requirements for a non-power reactor are specified in 10 CFR 100 (referenced by 10 CFR 50.34(a)(1)(i)). Specifically, 10 CFR 100.11 sets the dose limits for siting a test (non-power) reactor. Consistent with the guidance in NUREG 1537, an MHA is used to demonstrate that the radiological consequences from a bounding event result in acceptable dose levels. The bounding nature of the MHA also provides the preliminary analysis of the facility and determination of the margin of safety during transient conditions required by 10 CFR 50.34(a)(4).

For a plant with more than one reactor unit, 10 CFR 100.11(b) requires consideration of the degree of independence between units in the dose evaluation. Evaluation of the degree of independence includes consideration of whether the reactors are independent to the extent that a postulated event for unit does not affect the safety of operation of the other unit.

© 2024 Kairos Power LLC

The final analysis of the facility and determination of the margin of safety during transient conditions is deferred to the final safety analysis report. Deferring the final safety analysis is consistent with the expectations in 10 CFR 50.35(a)(2) because the final design details and the technical information needed to complete a final safety analysis, such as validation testing, will not be submitted until the operating license application stage. To support a finding that the remaining portions of the safety analysis can reasonably be left to the final safety analysis report, the transient methodology is provided in this technical report, along with sample calculations to illustrate the methods and potential margins in the final safety analysis. However, the sample calculations are for illustration purposes only because Kairos Power is not requesting Commission approval of the safety of any design feature or specification in the construction permit application, as permitted by 10 CFR 50.35(b). The verification and validation plan for codes used in the safety analysis evaluation are also provided in this report, consistent with the expectation in 10 CFR 50.35(a)(3) and 10 CFR 50.35(a)(4).

The transient methodology presented in this report is consistent with the NUREG 1537 objectives for information on postulated events with the exception of guidance for “rejection of a potential event.” The potential event initiators prevented by design are provided in the Preliminary Safety Analysis Report. The objectives listed in NUREG 1537 are:

- *Ensure that enough events have been considered to include any accident with significant radiological consequences. Rejection of a potential event should be justified in the discussions.*
- *Categorize the initiating events and scenarios by type and likelihood of occurrence so that only the limiting cases in each group must be quantitatively analyzed.*
- *Develop and apply consistent, specific acceptance criteria for the consequences of each postulated event.*

The development of evaluation models (EMs) for safety analysis is consistent with the applicable portions of the evaluation model development and assessment process (EMDAP) described in RG 1.203, “Transient and Accident Analysis Methods”. A summary of the EMDAP is provided in Figure 1-1. This report follows the process for Elements 1 and 3. Elements 2 and 4 will be provided in a future licensing submittal to support a final safety analysis report.

© 2024 Kairos Power LLC

2 MAXIMUM HYPOTHETICAL ACCIDENT SUMMARY

2.1 MAXIMUM HYPOTHETICAL ACCIDENT NARRATIVE

The reactor is tripped due to an unspecified transient. Pre-transient diffusion of radionuclides from the fuel kernels are hypothetically and conservatively not modeled to maximize available fuel inventory release. The accident is detected by the reactor protection system, and the safety functions for reactor shutdown and decay heat removal are assumed to be fulfilled. However, the thermal fluid response is not directly modeled. Hypothetical temperature curves are used to bound expected system temperatures and thus conservatively drive radionuclide movement through the credited barriers:

- Radionuclides diffuse from all TRISO cohorts (e.g., intact, failed SiC, exposed kernels). This fuel release is hypothetical given the steady state diffusion assumptions.
- Tritium desorbs from in-vessel graphite and steel.
- Radionuclides evaporate and degas from the Flibe driven by natural convective forces in the cover gas.
- Non-gaseous radionuclides (i.e., Salt-soluble Fluorides, Noble Metals, and Oxides) evaporate from the Flibe free surface in the reactor vessel.
- Gaseous radionuclides, including tritium, bypass the Flibe.

Airborne radionuclides are conservatively assumed to bypass the cover gas space and directly enter the facility air. Radionuclides that have been mobilized in the facility air are then transported by dispersion to the site boundary on the basis of conservative analysis with unfiltered ground level releases.

2.2 MAXIMUM HYPOTHETICAL ACCIDENT TEMPERATURE CURVE

A time-temperature plot of the prescribed MHA system temperatures is shown in Figure 2-1 and Table 2-1. This temperature profile bounds the expected release from fuel, Flibe, and structural temperatures for postulated events.

2.3 CONSERVATIVE RELEASE MODELS

The calculation of the dose consequences of the MHA uses the source term methods for design basis accidents presented in Reference 3. This section provides a high-level summary of the methods used and the inputs to the calculation.

The evaluation of the MHA dose consequences first identifies and accounts for the sources of MAR and the barriers to release. Each barrier is then evaluated for a release fraction to provide dose consequences at the exclusion area and low population zone boundaries.

The evaluation of the MHA dose consequences first identifies and accounts for the sources of MAR and the barriers to release. Each barrier is then evaluated for a release fraction to provide dose consequences at the exclusion area and low population zone boundaries.
The four sources of MAR and the associated barriers to release in the MHA:

- TRISO fuel in the reactor core
    - Barriers: TRISO layers, Flibe, and gas space
- Circulating activity
    - Barriers: Flibe and gas space

© 2024 Kairos Power LLC

- Structural MAR
    - Tritium retained by graphite and in Flibe
        - Barriers: Graphite grains (for non-Flibe tritium) and gas space
    - Argon-41 retained in closed graphite pores
        - Barriers: Graphite pores and gas space

There are several non-physical conditions that are hypothesized to ensure a bounding MHA:

- Pre-transient diffusion of radionuclides from the fuel in the reactor core is neglected: This conservatism is achieved in the evaluation by assuming that the full radionuclide inventory of the fuel is available for release at the initiation of the MHA. The circulating activity is still assumed to be at an upper bound level. Therefore, any MAR originating in the fuel that contributes to the circulating activity is effectively double counted.
- Hypothetical temperature histories are applied to the transient: the hypothetical temperature histories applied to the MHA is provided in Figure 2-1. These temperatures set an upper limit for the figure of merit temperatures in the postulated events.
- The gas space is not credited for confinement of the radionuclides that release from the Flibe free surface: radionuclide transport in the gas space barrier is modeled using the conservative building transport and off-site dispersion methods described in Reference 3.
- Conservative, unfiltered, ground level releases: the gas space transport evaluation assumes a conservative leakage rate for the reactor building that releases the entire volume within a 2-hour window as the building is assumed to not be a confinement structure. The dispersion evaluation assumes no radionuclides are filtered after the building transport is evaluated to avoid taking credit for any radionuclide filtering that could occur in the heating, ventilation, and air conditioning system.
- Initial tritium inventories are calculated for an assumed 50 MWth core that operates at a 100% capacity factor over ten years. The reactor is expected to operate at lower powers with a lower capacity factor. Lower operating powers result in a lower tritium production rate and lower capacity factors allow for the graphite grains to experience time periods of tritium desorption instead of sorption.
- A bounding vessel void fraction of 0.1 is assumed to facilitate the release of low volatility species in the vessel via bubble burst.

Quantification of MAR Sources

The fuel MAR consists of radionuclides produced by normal operation. A Serpent2 evaluation provides the fuel inventory. The fuel MAR is assumed to transport in the radionuclide groups described in Reference 3.

A bounding value of circulating activity is assumed for Flibe MAR in the analysis. The Flibe MAR is assumed to transport in the groups described in Reference 3.

The quantity of retained tritium is conservatively bound within graphite and structures over 10 years of operation. The tritium T speciation is simplified to fully tritium fluoride for an oxidizing salt. A fully molecular tritium case for a reducing salt is calculated, but the fully tritium fluoride case is used because

© 2024 Kairos Power LLC

it leads to a higher graphite inventory and higher total release of tritium. The tritium fluoride is assumed to be retained by the graphite, but does not permeate, and its evolution to off-gas is neglected. The tritium fluoride distribution is determined by mass transfer in Flibe, where the graphite is treated as a perfect absorber. Distribution fractions to each region are calculated by mass transfer coefficient multiplied by the surface area. The mass transfer coefficients are calculated by the correlations in Reference 3. Once the transient begins, the concentration of tritium in the Flibe is reduced to zero and thus the concentration gradient reverses, moving tritium out of grains and back into the Flibe. Tritium release fractions are calculated using a numerical solution to diffusion equations. The tritium transport through graphite pores is assumed to be instantaneous, and graphite grains are exposed to the same tritium uptake conditions. Strong tritium trapping sites are neglected to bound release fractions.

The Ar-41 buildup and release models predict the diffusion of argon cover gas into graphite closed pores which are then activated in the core and reflector regions. Graphite used for the reflector as well as carbon matrix used for fuel and moderator pebbles are porous materials. Small entrance pore sizes of the graphite prevent salt intrusion into the bulk material, and the volume of pores is available for occupancy by a gas. The closed porous volume of graphite and carbon matrix is occupied by the cover gas for the reactor. Cover gas also diffuses through the Flibe and enters graphite closed pores during reactor operations since argon cover gas has small, but non-zero solubility in Flibe. The inventory of Ar-41 is assumed to be puff released directly into the gas space.

Radionuclide Transport in Fuel

The grouped fuel MAR diffuses through the TRISO layers, driven by the hypothetical temperature history in Figure 2-1. As discussed in Reference 3, the transport of mobile radionuclides through the TRISO fuel particle is modeled by Fick's laws of diffusion.

No further generation of radionuclides occurs after the reactor trip. Additionally, no radioactive decay is modeled in the mass diffusion equations. The short-time approximation of the Booth solution is used to determine the fractional release of radionuclides from the kernel for conditions where $\tau \leq 0.155$ (no power, no further generation of nuclides) (Reference 4):

$$RF(t = T) = 6\sqrt{\frac{\tau}{\pi}} - 3\tau \quad (1)$$

where,

RF(T) = release fraction of radionuclides up to time $t=T$

τ = reduced diffusion coefficient = DT/a^2 (unit-less)

a = radius of equivalent sphere (m)

D = diffusivity coefficient of the representative radionuclide (m^2/s), consistent with the values in Reference 3.

© 2024 Kairos Power LLC

t = time (s)

For conditions where $\tau \geq 0.155$ and radioactive decay are ignored, the long-time approximation for release fraction for the kernel is modeled as (Reference 5):

$$RF(t = T) = 1 - \frac{6}{\pi^2} e^{-\pi^2 \tau} \quad (2)$$

The short time approximation for fractional release of a coating layer is (Reference 6):

$$RF(T) \approx \frac{24\gamma(1+\gamma)}{\sqrt{\pi}} e^{-\frac{1}{4\tau}} \tau^{1.5} [1 - 6\tau(1+\gamma) + 12\tau^2(5 + 6\gamma + 6\gamma^2)] \quad (3)$$

where,

RF(T) = release fraction of radionuclides up to time t=T

γ = ratio of layer thickness to the inner radius of the layer (unit-less)

τ =reduced diffusion coefficient= $\frac{DT}{d^2}$ (unit-less)

D = diffusivity of the diffusing species in the diffusing medium (m^2/s), consistent with the values in Reference 3.

t = time (s)

d = thickness of the coating layer (m)

This short time approximation is applied to conditions where $\tau \leq 0.2$. When $\tau > 0.2$, the following long time approximation equation is used to calculate the fractional release for a coating layer (Reference 6):

$$RF(t) \cong 1 - (1 + \frac{\gamma}{2}) e^{-3\gamma\tau} \quad (4)$$

Radionuclide diffusion through TRISO layers is employed for fuel release assuming no depletion of the radionuclide inventory due to operation time. In this bounding model, radionuclides are assumed to continuously challenge each barrier independent of quantity of radionuclides actually challenging a barrier at any given time. For example, radionuclides that reach the outer pyrolytic carbon (OPyC) layer at day five of the simulation would instantly be released from the OPyC layer with a fraction equivalent to radionuclides that have been diffusing through the barrier since the initiation of the transient. The release fraction (RF) of compromised layers is conservatively set to 1.0.

© 2024 Kairos Power LLC

$$RF_{fuel}^{i}(t=T) = \prod_{j=kernel}^{OPyC} RF_{j}^{i}(t=T) \tag{5}$$

Structural MAR Transport from Structural Materials

The tritium is released from the system in the following batches which roughly corresponds to the X/Q dispersion bins:

1) "Puff" release of tritium in both the Flibe and pebble carbon matrix, due to the high diffusivities at the prescribed pebble carbon matrix temperatures, at the beginning of the transient
2) A bounding diffusion model estimates the fraction of tritium that transports out of reflector graphite grains from:
   i. 0 to 10 min
   ii. 10 min to 2 hours
   iii. 2 hours to 8 hours
   iv. 8 hours to 14 hours
   v. 14 hours to 24 hours
3) Remaining tritium in the system transports out of the system by an assumed "puff" release 24 hours into the transient

All Ar-41 predicted to be contained within graphite structures at the initiation of the transient is "puff" released into the gas space.

Transport of MAR from Flibe to the Gas Space

The two release mechanisms for MAR in the circulating Flibe are bubble burst from entrained cover gas in the vessel coolant and evaporation driven by the MHA temperature curve. Bubble burst occurs before transient diffusion can occur from the fuel into the Flibe, but evaporation mobilizes both circulating activity and MAR that has diffused from the fuel into the Flibe.

For a two-phase flow, the void fraction of the flow is designated by α. The volumetric flow rate of gas $Q_{g,2p}$ is related to the two-phase mass flow rate of Flibe $W_{f,2p}$ by the following expression:

$$Q_{g,2p} = \frac{W_{f,2p}}{\rho_f}\frac{\alpha}{1-\alpha} \tag{6}$$

The aerosol generation rate $W_{a,2p}$ is obtained through the volumetric ratio E_a(the ratio of the volume of particles generated by a single bubble bursting to the volume of the bubble) as:

© 2024 Kairos Power LLC

$$W_{a,2p} = \rho_f E_a Q_{g,2p} = W_{f,2p} E_a \frac{\alpha}{1-\alpha} \quad (7)$$

The bounding value of E_a = 2.1 x 10^{-6} is chosen for the Flibe-argon system.

For conservatism, no deposition is assumed during the aerosol generation process. The total mass of aerosol is given by:

$$m_{a,2p} = \int_0^t W_{a,2p} dt = m_{f,2p} E_a \frac{\alpha}{1-\alpha} \quad (8)$$

where $m_{f,2p}$ is the mass of two-phase Flibe. Thus, the aerosol release fraction from bubble burst is calculated using:

$$ARF_{2p} = E_a \frac{\alpha}{1-\alpha} \quad (9)$$

The release rates for gases and high volatility noble metals in the circulating activity are conservatively bounded by instantaneous (or "puff") releases at the beginning of the transient. Other radionuclides release from the Flibe at a rate determined by the general evaporation law, as described in Reference 3. Conservative mass transfer coefficients that neglect liquid side mass transfer resistance are used.

The radionuclides evaporated from the Flibe free surface are separated into the following release inventories:

1) "Puff" release of dissolved noble gases and bubble burst Flibe aerosols at the beginning of the transient;
2) One linear release for evaporation of radionuclides over the first 10 min temperature interval corresponding to pre-reactor trip fuel temperature;
3) One linear release for evaporation of radionuclides over the next 110 min temperature interval;
4) One linear release for evaporation of radionuclides over the 70-hour release interval;
5) One linear release per day for the next seven days for the reactor cool down period; and
6) One final linear release over the 20 days.

Gas Space

The gas space transport evaluation is divided into two models: building transport and atmospheric dispersion. The methodology for Design Basis Accidents in Reference 3 is used to evaluate the gas space transport. Site-specific $\frac{\chi}{Q}$ values are used as input to the dispersion modeling.

© 2024 Kairos Power LLC

2.4 RESULTS

The MHA summarized in this report results in doses that are well below the 10 CFR 100 limits for non-power reactor siting and below the Environmental Protection Agency Guideline guidance for protection actions. Acceptance criteria for figures of merit that are surrogates for radionuclide releases for the various postulated event categories are derived from the MHA conditions to ensure that postulated events are bounded by the MHA as discussed in Section 3.4.

© 2024 Kairos Power LLC

3 CAPABILITY OF EVALUATION MODELS

3.1 OVERVIEW OF EVALUATION MODELS FOR POSTULATED EVENTS

The safety analysis of postulated events requires the use of several EMs. This section describes the capability of the evaluation models by providing the list of postulated events that the EMs are used to analyze, the important phenomena that must be captured by the EMs, and the figures of merit that must be evaluated by the EMs.

3.2 EVALUATION MODEL APPLICABILITY

3.2.1 Postulated Event Categories and Duration of Evaluation

The postulated events include any potential upset to plant operations, within the plant design basis, that causes an unplanned transient to occur. The effects of postulated events are mitigated by design features. Any event excluded (prevented by design) must be described in the licensing application. Consistent with NUREG 1537, the postulated events with similar characteristics and modeling approaches are grouped into categories. The postulated events are grouped into the following categories:

- Salt Spills
- Insertion of Excess Reactivity
- Increase in Heat Removal
- Loss of Forced Circulation (Loss of Normal Electrical Power events are bounded by this event group)
- Internal Hazard Events
- External Hazard Events
- Pebble Handling and Storage System Malfunction
- Intermediate Heat Exchanger Tube Break
- Radioactive Release from a Subsystem or Component
- General Challenges to Normal Operation

The limiting event for each category is analyzed from the event initiation until the plant reaches a safe state. The safe state is defined for each category of events as a point where the transient figures of merit have stabilized in a safe condition. For any events that occur when fuel is loaded in the core, the plant must be in a safe shutdown condition, where the control and shutdown elements insert to shut down the reactor and maintain long term reactivity control, and the decay heat is removed either through parasitic heat losses, or by the decay heat removal system. The decay heat removal system (DHRS) is always on when the anticipated reactor decay heat load is greater than parasitic heat loss. Similar to other passive reactor designs, the reactor relies on passive heat removal that does not require operator intervention to mitigate the heat up effects of postulated events. Therefore, the transient methods for each category of postulated event require that an analysis shows the event reaches and maintains a safe state for at least 72 hours following the initiation of the transient. The time during which the decay heat removal system is relied upon to mitigate the heat up effects of an event is referred to as the mission time.

3.2.2 Postulated Events

© 2024 Kairos Power LLC

This section provides a narrative description of each postulated event category. In each category, the narrative is accompanied by the event-specific characteristics that define a safe state, and the figures of merit that the design is evaluated against to ensure the limiting postulated event for the category remains bounded by the MHA. The general narrative for each postulated event category is provided in this section to provide context for the figures of merit. The event-specific details and analysis methods are provided in Section 4.5.

3.2.2.1 Salt Spills

A hypothetical double-ended guillotine break in the primary salt piping during normal operation causes Flibe to spill from the primary heat transport system. Salt spills are detected directly or indirectly by the reactor protection system, which initiates control and shutdown elements insertion, fulfilling the reactivity control function. The primary coolant pump trip and anti-siphon features of the primary system limit the amount of spilled Flibe. The reactor decay heat removal system limits reactor temperature and fulfills the decay heat removal function. In the reactor, air that enters the reactor system from the break reacts with Flibe to form volatile products and oxidizes unsubmerged structural graphite and pebble carbon matrix of unsubmerged pebbles. A fraction of the radionuclides that are normally circulating in the Flibe are released into the facility air when aerosols are generated from the salt that exits the pipe. The Flibe spills onto the reactor cell floor and forms a pool. The reactor cell floor is assumed to be designed to preclude Flibe-concrete reactions. Additional radionuclides in the spilled Flibe are released through evaporation until the top surface of the Flibe pool is solidified.

A safe state is established when:

- The core is subcritical and long-term reactivity control is assured.
- The decay heat is being removed and long-term cooling is assured, where figures of merit temperatures are steadily decreasing during the mission time of the decay heat removal system.
- Flibe temperature inside the reactor vessel remains above the Flibe freezing temperature.
- Flibe stops spilling out of the break and the resulting Flibe pool freezes.

This narrative captures the limiting event of this postulated event category. Other events grouped in this category include:

- Spurious draining and smaller leaks from the primary heat transport system
- Leaks from other Flibe containing systems and components (e.g., inventory management system fill/drain tank, inventory management system piping, chemistry control system piping, heat rejection radiator [HRR] tube)
- Leaks up to the hypothetical double-ended guillotine primary salt piping break size
- Mechanical impact or collision events involving Flibe containing structures, systems, and components (SSCs) (except the vessel)
- Leaks from the intermediate heat transport system that contains a non-Flibe coolant, which may contain a non-zero amount of radionuclides

The pipe break on the hot leg is assumed to be the limiting scenario. However, the event-specific methods in Section 4.5 describe a spectrum of break sizes and scenarios is analyzed to confirm the bounding salt spill event. The break sizes and locations determine the amount of mechanical aerosol

© 2024 Kairos Power LLC

generated by the spilled Flibe jet. After the pipe break is detected by the reactor protection system and trips the reactor, the response of the core is similar for other break sizes.

For pipe break scenarios in other Flibe containing SSCs (except the vessel) not connected to the reactor, the core does not experience a transient from reactor trip.

In order to ensure that the design features mitigating a salt spill event are sufficient to keep the consequences bounded by the MHA, the following key figures of merit must be evaluated:

- Peak TRISO temperature to limit diffusion of radionuclides
- TRISO failure probability to limit incremental TRISO layer failures
- Peak Flibe-cover gas interfacial temperature to limit evaporation mass transfer of radionuclides
- Peak vessel and core barrel temperatures to prevent vessel failure and maintain long term cooling
- Aerosols generated by released Flibe to limit the materials at risk released
- Volatile products formed from the chemical reaction between Flibe and air, Flibe and stainless steel, and Flibe and insulation to limit the materials at risk released
- Mass loss of structural graphite due to oxidation to limit tritium release
- Mass loss of pebble carbon matrix due to oxidation to limit tritium release and prevent additional release of materials at risk
- Peak temperature of structural graphite to limit the tritium release
- Peak temperature of pebble carbon matrix to limit the amount of tritium release

3.2.2.2 Insertion of Excess Reactivity

A control system error or operator error causes a continuous withdrawal of the highest worth control element at maximum reactivity control and shutdown system (RCSS) drive speed. The reactivity insertion is detected by the reactor protection system which initiates control and shutdown elements insertion, fulfilling the reactivity control function. The reactor decay heat removal system limits reactor temperature and fulfills the heat removal function.

A safe state is established when:

- The core is subcritical and long-term reactivity control is assured.
- The decay heat is being removed and long-term cooling is assured, where figures of merit temperatures are steadily decreasing during the mission time of the decay heat removal system.
- Flibe temperature inside the reactor vessel remains above the Flibe freezing temperature.

This narrative captures the limiting event of this postulated event category. Other events grouped in this category include:

- Reactivity insertion events caused by fuel loading error (e.g., errors in rate of fresh fuel injection, incorrect order of fuel insertion)
- Reactivity insertion events with concurrent pump trip
- Reactivity insertion events with normal heat removal available

© 2024 Kairos Power LLC

- Local phenomena leading to ramp insertion of reactivity
- Change in reactivity due to shifting of graphite reflector blocks
- Venting of gas bubbles accumulated in the active core
- Local phenomena leading to step insertion of reactivity
- Local negative reactivity anomaly (e.g., inadvertent single element insertion, cover gas injection)
- Reactivity insertion events during startup

The control element withdrawal at maximum speed, described above, is assumed to be the limiting event of this category. However, the amount and rate of reactivity insertion from other grouped events under insertion of excess reactivity (e.g., during the pebble loading error event, venting of accumulated gas bubbles in the active core) is compared with those from the control element withdrawal events. Additionally, the reactivity insertion due to Increase in Heat Removal events and design basis seismic event, respectively, is compared to the reactivity insertion of control element withdrawal events.

In order to ensure that the design features mitigating a reactivity insertion event are sufficient to keep the consequences bounded by the MHA, the following key figures of merit must be evaluated:

- Peak TRISO temperature to limit diffusion of radionuclides
- TRISO failure probability to limit incremental TRISO layer failures
- Peak Flibe-cover gas interfacial temperature to limit evaporation mass transfer of radionuclides
- Peak vessel and core barrel temperatures to prevent vessel failure and maintain long term cooling
- Peak temperature of structural graphite to limit the tritium release
- Peak temperature of pebble carbon matrix to limit the amount of tritium release

3.2.2.3 Increase in Heat Removal

The primary coolant pump overspeeds, causing a surge insertion of cold Flibe into the core. The event is detected by the reactor protection system, which initiates control and shutdown elements insertion, fulfilling the reactivity control function. The reactor protection system also trips the primary coolant pump. The reactor decay heat removal system limits reactor temperature and fulfills the heat removal function.

A safe state is established when:

- The core is subcritical and long-term reactivity control is assured.
- The decay heat is being removed and long-term cooling is assured, where figure of merit temperatures are steadily decreasing during the mission time of the decay heat removal system.
- Flibe temperature inside the reactor vessel remains above the Flibe freezing temperature.

This narrative captures the limiting event of this postulated event category. Other events grouped in this category include:

- Increase in heat removal due to overspeed of heat rejection blower or intermediate salt pump
- Increase in heat removal during low power operation

© 2024 Kairos Power LLC

- Spurious actuation of PHTS normal decay heat removal heat rejection radiator
- Spurious opening of a turbine bypass valve or steam safety valve
- Superheater shell leak
- Steam line break

The increase in heat removal events are demonstrated to be bounded by the insertion of excess reactivity postulated event.

In order to ensure that the design features mitigating an increase in heat removal event are sufficient to keep the consequences bounded by the MHA, the following key figures of merit must be evaluated:

- Peak TRISO temperature to limit diffusion of radionuclides
- TRISO failure probability to limit incremental TRISO layer failures
- Peak Flibe-cover gas interfacial temperature to limit evaporation mass transfer of radionuclides
- Peak vessel and core barrel temperatures to prevent vessel failure and maintain long term cooling
- Peak temperature of structural graphite to limit the tritium release
- Peak temperature of pebble carbon matrix to limit the amount of tritium release

3.2.2.4 Loss of Forced Circulation

The failure of the primary salt pump results in the loss of forced circulation. The reduced flow is detected directly or indirectly by the reactor protection system, which initiates control and shutdown elements insertion, fulfilling the reactivity control function. The reactor decay heat removal system limits reactor temperature and fulfills the heat removal function.

A safe state is established when:

- The core is subcritical and long-term reactivity control is assured.
- The decay heat is being removed and long-term cooling is assured, where figures of merit temperatures are steadily decreasing during the mission time of the decay heat removal system.
- Flibe temperature inside the reactor vessel remains above the Flibe freezing temperature.

This narrative captures the limiting event of this postulated event category. Other events grouped in this category include loss of forced circulation due to:

- Blockage of flow path external to the reactor vessel in the primary heat transport system,
- Spurious pump trip signal
- Pump seizure
- Shaft fracture
- Bearing failure
- Pump control system errors
- Supply breaker spurious opening
- Loss of net-positive suction head (e.g., pump overspeed, low level)

© 2024 Kairos Power LLC

- Loss of normal electrical power
- Flibe freezing inside heat rejection radiator tubes
- Loss of normal heat sink (e.g., ISP failure, superheater tube rupture)

There are two bounding events within this event category to evaluate the long-term passive cooling performance. One is to bound the overheating consequence, and another is to bound the downcomer freezing consequence. Two scenarios are considered for these two bounding events:

- The first event scenario (overheating) considers the limiting case to analyze the peak vessel and core barrel temperatures to prevent vessel failure and maintain coolable geometry. The most limiting reactor operation power and operating history are assumed.
- The second scenario (long-term overcooling) aim at the reactor performance evaluation in terms of coolant freeze prevention at downcomer. A spectrum of reactor decay heat levels and operating power levels are analyzed for this purpose.

For the overheating bounding event, the loss of forced circulation due to loss of normal electrical power is bounded by the primary salt pump failure scenario. The loss of power to the reactivity control and shutdown system mechanisms results in release and insertion of the control and shutdown elements. As such, the reactor power is reduced faster compared to other loss of forced circulation scenarios where the reactor trips on a reactor trip signal. For the long-term overcooling bounding event, the loss of normal electrical power event bounds other loss of circulation scenarios since this event has the least stored energy.

In order to ensure that the design features mitigating a loss of forced circulation event are sufficient to keep the consequences bounded by the MHA, the following key figures of merit must be evaluated:

- Peak TRISO temperature to limit diffusion of radionuclides
- TRISO failure probability to limit incremental TRISO layer failures
- Peak Flibe-cover gas interfacial temperature to limit evaporation mass transfer of radionuclides
- Peak vessel and core barrel temperatures to prevent vessel failure and maintain long term cooling
- Peak temperature of structural graphite to limit the tritium release
- Peak temperature of pebble carbon matrix to limit the amount of tritium release

The only figure of merit for the long-term overcooling scenario is:

- Minimum reactor vessel inner surface temperature to prevent partial freezing within downcomer

3.2.2.5 Pebble Handling and Storage System Malfunction

There are three types of events in this event category: pebble handling and storage system (PHSS) break, loss of PHSS cooling, and grinding of a pebble in the pebble handling machine. However, the loss of PHSS cooling is an event mitigated through design of pebble storage system, and the grinding of pebble mitigated through the design of pebble extraction machine. The consequences of these two events are expected to be limited by the design specifications which are bounded by MHA consequence. Therefore, the PHSS break event is the assumed limiting event to be analyzed for this category.

© 2024 Kairos Power LLC

The pebble handling and storage system transfer line breaks when pebbles are getting removed from the core, resulting in spilling of the pebbles within the transfer line into the reactor cell. This condition is detected directly or indirectly by the reactor protection system, which trips the pebble handling and storage system to stop pebble movement. For the spilled pebbles, the reactivity control function is fulfilled by the low fissile inventory of pebbles, which precludes criticality safety concerns, while heat transfer mechanisms within the room fulfills the heat removal function. The structural integrity of the pebbles maintains the confinement function. For the pebbles remaining in the pebble handling and storage system, the reactivity control, heat removal and confinement functions continue to be fulfilled by the system design resulting in a safe and stable state. The heat up of the pebbles in the PHSS mobilizes the Flibe accumulated on the piping. Air ingress into the PHSS and reactor cover gas region occurs through the break.

A safe state is established when:

- The movement of pebbles outside of the core has stopped and criticality safety is assured.
- Decay heat is being removed from pebbles outside of the core and long-term cooling is assured, where figure of merit temperatures are steadily decreasing.

This narrative captures the limiting PHSS break event of this postulated event category. Other PHSS break events grouped in this category include:

- A transfer line break when pebbles are getting inserted into empty core
- A transfer line break when pebbles are getting inserted into the core at power
- A transfer line break when pebbles are getting transferred to storage canisters
- A mishandling of fuel outside the reactor (e.g., containment box, at the material balance areas and key measure points)

The PHSS break event when pebbles are extracted from the core is considered bounding among the grouped events because the spilled pebbles have higher temperatures and burnups, therefore, the highest decay heat and MAR loading compared to other events in the group.

In order to ensure that the design features mitigating a PHSS break event are sufficient to keep the consequences bounded by the MHA, the following key figures of merit must be evaluated:

- Peak TRISO temperature ex-vessel to limit diffusion of radionuclides
- Mobilized Flibe and graphite dust released
- Peak TRISO temperature in vessel to limit diffusion of radionuclides
- TRISO failure probability to limit incremental TRISO layer failures
- Peak Flibe-cover gas interfacial temperature to limit evaporation mass transfer of radionuclides
- Peak vessel and core barrel temperatures to prevent vessel failure and maintain long term cooling
- Mass loss of pebble carbon matrix due to oxidation to limit tritium release and prevent additional release of materials at risk
- Mass loss of structural graphite due to oxidation to limit tritium release
- Peak temperature of structural graphite to limit the tritium release

© 2024 Kairos Power LLC

- Peak temperature of pebble carbon matrix to limit the amount of tritium release

3.2.2.6 Radioactive Release from a Subsystem or Component

An external hazard event causes components not protected from the hazard to fail and release MAR stored in these systems. These systems include:

- Tritium management system
- Inert gas system
- Chemistry control system
- Inventory management system
- Intermediate heat transport system
- Power generation systems

This narrative captures the limiting event of this postulated event category. Other events grouped in this category include:

- Individual boundary breaches or leaks from any of the above systems due to internal hazards or random failure
- Radioactive release from SSCs (e.g., residual Flibe in the primary salt pump (PSP), dust in PHSS piping) isolated for maintenance

The key figure of merit for this event is:

- Amount of materials at risk released

The limiting event for this category is assumed to be a seismic event that results in the failure of all systems or components not qualified to maintain structural integrity in a safe shutdown earthquake. The amount of MAR in these systems is assumed to be limited to an upper bound limit such that the total amount of material at risk released is bounded by the amount released during the MHA. Therefore, no additional transient analysis is needed.

3.2.2.7 Intermediate Heat Exchanger Tube Break

A complete break of one intermediate heat exchanger (IHX) tube occurs. The positive pressure difference maintained between the primary loop and intermediate loop forces the primary Flibe coolant into the intermediate loop and mixes with the intermediate salt coolant. The symptoms of the tube break are detected by the reactor protection system which initiates control and shutdown elements insertion, fulfilling the reactivity control function. The highest worth element is stuck out and does not insert. The reactor protection system also initiates primary coolant pump and intermediate coolant pump trips to limit BeNaF ingress into the reactor vessel. The reactor decay heat removal system performs its function to limit reactor temperature and fulfill the heat removal function. A conservative amount of Flibe is assumed to flow into the intermediate loop to mix with the intermediate salt. This amount is assumed to be the same or bounded by the volume of Flibe spill during a postulated pipe break event. The core response and dose consequence due to loss of Flibe into the intermediate loop during an intermediate heat exchanger tube break is bounded by those of a pipe break during salt spill postulated event. Small leaks in the IHX will be detected via limits on allowable leak threshold (e.g.,

© 2024 Kairos Power LLC

radioactivity measurement in the intermediate salt). The plant control system shuts down the reactor to mitigate the leaks.

A safe state is established when:

- The core is subcritical and long-term reactivity control is assured.
- The decay heat is being removed and long-term cooling is assured, where figures of merit temperatures are steadily decreasing during the mission time of the decay heat removal system.
- Flibe temperature inside the reactor vessel remains above the Flibe freezing temperature.
- The Flibe leak from the primary loop into the intermediate loop is contained

This narrative captures the limiting event of this postulated event category. Other events grouped in this category include:

- IHX tube leak

The intermediate heat exchanger tube break events are demonstrated to be bounded by the salt spill postulated event.

In order to ensure that the design features mitigating an intermediate heat exchanger tube break event are sufficient to keep the consequences bounded by the MHA, the following key figures of merit must be evaluated:

- Peak TRISO temperature to limit diffusion of radionuclides
- TRISO failure probability to limit incremental TRISO layer failures
- Peak Flibe-cover gas interfacial temperature to limit evaporation mass transfer of radionuclides
- Peak vessel and core barrel temperatures to prevent vessel failure and maintain long term cooling
- Aerosols generated by released Flibe to limit the materials at risk released
- Peak temperature of structural graphite bounded to limit the tritium release
- Peak temperature of pebble carbon matrix to limit the amount of tritium release

These figures of merit are also evaluated in the salt spill category. Therefore, this event could be grouped under the salt spill category.

3.2.2.8 Internal and External Hazards

The internal hazard events in the design basis include:

- Internal fire
- Internal water flood
- Turbine missile
- High energy steam line break

The external hazard events in the design basis include:

- Seismic event
- High wind event

© 2024 Kairos Power LLC

- Toxic release
- Mechanical impact or collision with SSCs
- External flood

The reactor can be shutdown manually (e.g., during a toxic release) or automatically (e.g., water flood causing a loss of electrical power). The decay heat removal system performs its function to limit reactor temperature and fulfill the heat removal function.

The key figures of merit for internal and external hazard events are

- The SSCs associated with engineered safety features are available to mitigate the events.
- The amount of materials at risk in SSCs not protected from the hazard are limited.

Engineered safety features contained within areas protected from or able to withstand the intensity of the hazard loading for hazard events initiated outside those areas (e.g., fire) maintain their capability to bring the plant to a safe state following a postulated event. The SSCs within those areas are designed to withstand an upper bound hazard loading intensity associated with the area (e.g., SSCs can withstand an upper bound heat load and the associated area is equipped with fire detection and suppression systems to limit the heat load).

A turbine missile could be generated due to a postulated turbine generator failure. Due to the favorable orientation of the turbine generator with respect to the reactor building, SSCs associated with engineered safety features are not affected by a potential turbine missile to the extent that they could not perform their safety functions.

For SSCs not protected with such an area, the amount of materials at risk are assumed to be limited to an upper bound limit such that the amount of materials at risk released is bounded by the amount released during the MHA.

During a seismic event, the packing fraction of the pebble bed would increase due to shaking of the pebble bed, and the graphite reflector blocks would shift. This results in an increase in reactivity, causing an increase in fuel temperature. The increase in reactivity due to increase in packing fraction of the pebble bed and maximum displacement of graphite reflector blocks during a seismic event is bounded by the insertion of excess reactivity event where the control element is inadvertently withdrawn. Increase in packing fraction in the core is equivalent to removal of Flibe which is a negative reactivity impact. The overall carbon-to-heavy-metal atom ratio (C/HM) stays fairly constant within the core. However, on the periphery of the bed close to the reflector, the C/HM is higher than the bed itself. This causes a situation where the reduction in that C/HM brings about a positive reactivity insertion in the core. Neutronics models with various packing fractions (lattice models) is used to demonstrate that the impacts are small.

Mechanical aerosols could also be generated due to splashing of Flibe in the reactor during a seismic event. The amount of aerosol generated during a seismic event is bounded by the amount of aerosol generated by the salt spill event where a pipe breaks.

A break in a high energy steam line could occur in the turbine generator building. Physical separation of the power generation systems from safety-related SSCs and the design of the safety-related portion of the reactor building ensures that a high energy break will not prevent safety-related SSCs from

© 2024 Kairos Power LLC

performing their safety functions. The potential reactivity insertion caused by an increase in heat removal due to a steam line break is considered in Section 3.2.2.3.

3.2.2.9 General Challenges to Normal Operation

A general challenge to normal operation occurs that requires an automatic or manual shutdown of a reactor unit. The disturbance is detected directly or indirectly by the reactor protection system, which initiates control and shutdown elements insertion, fulfilling the reactivity control function. The reactor decay heat removal system performs its function to limit reactor temperature and fulfill the heat removal function.

Grouped events include spurious trips due to control system anomalies, operator errors, and equipment failures. This event group also includes scenarios where operators choose to manually shutdown a reactor unit. Also included are faults in the reactivity control and shutdown system, electrical system, intermediate heat transport system, and other plant systems that would challenge normal operations.

This group also contains inert gas system disturbances, and instrumentation and control (I&C) faults. This event group is bounded by the Loss of Forced Circulation postulated event.

3.2.3 Evaluation Models Used to Analyze Postulated Events

Table 3-1 provides the list of postulated event categories, and the EM used to analyze them. Not all postulated events grouped in the categories are explicitly analyzed with the EMs described in this report. Section 4.5 describes the event-specific analysis methodology, which in some cases provides the justification for a postulated event or a postulated event category being bounded by a more limiting postulated event.

3.3 PHENOMENA IDENTIFICATION AND RANKING TABLES

The Phenomena Identification and Ranking Table (PIRT) process is an integral part of the Evaluation Model Development and Assessment Process laid out in RG 1.203. A PIRT relies on expert judgment to identify and rank key phenomena for a specific system undergoing a specific time phase of a specific transient. The PIRT process generates a prioritized list of key phenomena that need to be characterized and modeled to predict response to specific transients. It also ranks the knowledge level for each key phenomenon for each component, thus identifying critical gaps in the understanding of specific phenomena.

Kairos Power has performed a series of PIRTs for KP-FHRs. The list of PIRTs relevant to the development of safety analysis EMs, which leverage different sets of panel experts, include:

- Thermal fluids PIRT
- Radiological source term PIRT (Summary provided in Reference 3)
- Fuel Element PIRT (Summary provided in Reference 7)
- Neutronics PIRT (Summary provided in Reference 8)
- High-temperature structural materials PIRT (Summary provided in Reference 9)

The thermal fluids PIRT was performed to identify key thermal hydraulics phenomena important to safety, prioritize thermal hydraulics tests and EM development. The PIRT helps inform which areas of the EMs require existing data or testing to validate. Ultimately, the PIRT is a tool that helps inform the safety analysis methodology development and assessment of overall evaluation model adequacy.

© 2024 Kairos Power LLC

Key phenomena relevant to postulated events that were identified as having a high importance to safety and a low knowledge level for postulated events are summarized in the following list, and will be addressed with model development or/and validation tests:

- [[

]]

3.4 FIGURES OF MERIT

3.4.1 Dose Acceptance Criteria

The dose consequences of the MHA demonstrate the acceptability of the design when compared to regulatory dose limits. There are no dose limits defined in 10 CFR 50 for a test reactor; 10 CFR 100 defines dose limits applicable to a test reactor. The dose limits in 10 CFR 100.11 require that an applicant for a test reactor evaluate dose at the EAB and the low population zone (LPZ) as follows:

- EAB: An individual located on the EAB for two hours immediately following onset of the postulated fission product release would not receive a total radiation dose to the whole body in excess of 25 rem or a total radiation dose in excess of 300 rem to the thyroid from iodine exposure.
- LPZ: An individual located on the outer boundary of the LPZ who is exposed to the radioactive cloud resulting from the MHA (during the entire period of its passage) would not receive a total radiation dose to the whole body in excess of 25 rem or a total radiation dose in excess of 300 rem to the thyroid from iodine exposure.

The MHA described in Section 2 results in a bounding dose consequence for a KP-FHR with design features described in Section 1 that are significantly lower than those specified in 10 CFR 100.11. Specifically, the MHA results in a whole-body dose at the site boundary that is less than 1 rem.

3.4.2 Postulated Event Figures of Merit

Three methods are available to ensure and demonstrate a postulated event is bounded by the MHA: (1) direct dose calculation for all release pathways, (2) using figures of merit as surrogate for dose, and (3) using both direct dose calculation for some release pathways and figures of merit for other pathways. Direct dose calculation is the most straight forward method; however, it requires complex analysis. Figures of merit method can significantly reduce analysis cost since the dose of the same release pathway can be bounded by one bounding case.

© 2024 Kairos Power LLC

Figures of merit for the postulated event must be demonstrated to meet acceptance criteria derived from the MHA conditions. The figures of merit for each postulated event are developed based on the release pathways of radionuclides during the event. The acceptance criteria for figures of merit are developed to ensure the radionuclide releases from the postulated events through the same pathways as the MHA are less than those from the MHA. Therefore, if the acceptance criteria for all figures of merit for a postulated event are met, the dose of the postulated event is bounded by the MHA.

For the postulated events with additional release pathways that do not exist in the MHA, the third method is used. This method has three steps:

1. Bounding doses are calculated for each release pathway; bounding dose for each release pathway is then used to derive acceptance criteria for figures of merit according to the bounding release pathway conditions for the postulated event.
2. For each specific postulated event, if figures of merit for the involved release pathways meet acceptance criteria, the corresponding bounding dose values for the pathways can be used instead of direct dose analysis. Direct dose analysis for certain release pathways can also be performed.
3. All the dose values for each release pathway for the postulated event are summed to compare with the MHA total release dose. The total dose for the postulated event must be lower than the MHA dose.

As an example, for the figures of merit method (i.e., second method), during a core transient, radionuclides diffuse through the TRISO fuel layers as a function of temperature. Radionuclides in Flibe evaporate from the Flibe-cover gas interface as a function of temperature. Tritium desorbs from the graphite and pebble carbon matrix. Therefore, the peak TRISO temperature-time, peak Flibe-cover gas interfacial temperature, peak graphite temperature and peak pebble carbon matrix temperature profiles during the event are figures of merit for a postulated event that involves the core. Additionally, TRISO failure probability is also a figure of merit to limit incremental fuel failure to a negligible level during the transient; peak vessel and core barrel temperatures are key figure of merit to ensure the reactor vessel performs its safety function.

The figures of merit used for systems code analysis (KP-SAM) are a surrogate for demonstrating that consequences are bounded by MHA doses, or for maintaining a coolable geometry. However, if dose is the figure of merit for an event (i.e., a dose analysis is performed for the event), then those surrogate figures of merit for dose do not need to meet acceptance criteria, because the dose acceptance criterion is being explicitly evaluated. Likewise, when a figure of merit has been analyzed separately for bounding conditions (e.g., a structural analysis of the vessel is performed separately from the systems analysis) then that figure of merit does not need to be analyzed in the systems code to meet an acceptance criterion.

The figures of merit and associated acceptance criteria are provided in Table 3-2. The applicable event(s) are those that are expected to provide the limiting case for a given figure of merit.

3.4.2.1 Peak TRISO Temperature-Time

The release pathway for fuel is diffusional release as a function of temperature. During a postulated event, peak TRISO temperature is bounded by temperature-time curve derived from the assumed MHA fuel temperature-time curve to limit diffusion of radionuclides to less than the amount during the MHA.

© 2024 Kairos Power LLC

Bounding temperature-time curve derived from the assumed MHA temperature-time curve can be based on integrated effects on dose.

3.4.2.2 TRISO Failure Probability

Based on TRISO fuel qualification efforts as described in (Reference 26), it is expected that during a postulated event, incremental failure of TRISO fuel is limited to a negligible level if the peak temperature is below 1600°C. Failure probability of TRISO fuel can increase due to overpressure in the TRISO particles, which is a function temperature. The failure probability of TRISO fuel is evaluated using the methodology described in Section 4.2.

3.4.2.3 Peak Flibe-cover gas interfacial temperatures

Radionuclide release from Flibe is through evaporation. During a postulated event, peak Flibe-cover gas interfacial temperature is bounded by temperature-time curve derived from the assumed MHA Flibe-cover gas interfacial temperature-time curve to limit evaporation mass transfer of radionuclides to less than the amount during the MHA. Bounding temperature-time curve derived from the assumed MHA temperature-time curve can be based on integrated effects on dose.

3.4.2.4 Peak vessel and core barrel temperature

To prevent vessel failure and maintain long term cooling during a postulated event, the peak vessel and core barrel temperatures must be less than both (a) a maximum allowable temperature derived to limit excessive creep deformation and damage accumulation and (b) 750°C. The maximum allowable temperature is calculated so that the creep strain induced by primary membrane stresses within the vessel and the core barrel does not exceed 1% at the end of reactor life. Its derivation relies on the following assumptions:

- All regions of the vessel and core barrel in contact with Flibe are exposed to temperatures lower than or equal to 650°C for the hot operating time of the vessel and temperatures lower than or equal to the vessel and core barrel peak temperatures for a maximum duration of 360 hours (15 days).
- The maximum primary stresses undergone by the vessel and core barrel can be bounded by a maximum stress value derived as described in the evaluation model for structural integrity.

3.4.2.5 Minimum reactor vessel inner surface temperature

To ensure that the Flibe temperature within the vessel remains above the Flibe freezing temperature for at least 72 hours, a lower limit on the reactor vessel inner surface temperature is conservatively set to the Flibe freezing temperature.

3.4.2.6 Airborne release fraction of spilled/splashed Flibe

During a salt spill event, aerosols can be generated through jet breakup, and spilling and splashing. The airborne release fractions due to aerosolization must be limited so that the dose consequences of the salt spill events are bounded by the MHA.

3.4.2.7 Volatile products from Flibe chemical reactions

Flibe could be exposed to air during a salt spill event. The key release pathway of radionuclide from Flibe is through evaporation, which is a function of vapor pressure of the radionuclide species. When Flibe is exposed to air, the Flibe-air chemical reaction does not result in excessive reactive vaporization which would form radionuclide chemical species that have a higher vapor pressure than those already exists in

© 2024 Kairos Power LLC

Flibe circulating activity. It is expected that a few specific RN chemical species will have a higher vapor pressure after reacting with air than those in the circulating activity. However, those species are expected to be present at very low concentrations and the resulting difference in evaporation rate will be of minimal significance. For example, CsF dissolved in Flibe does not react with air to form a highly volatile cesium hydroxide. As such, Flibe-air reaction does not result in significant additional release of radionuclides from Flibe through evaporation.

The reactor cell floor is assumed to be designed to preclude Flibe-concrete reaction. When Flibe is spilled, it has the potential to come in contact with stainless steel and insulation material. Flibe interactions with stainless steel and insulation do not result in formation of radionuclide chemical species that have a higher vapor pressure than those already exists in Flibe circulating activity. Therefore, Flibe-stainless steel and Flibe-insulation reactions in the design basis do not result in additional release of radionuclides from Flibe through evaporation.

During a salt spill event, Flibe is not exposed to water, and therefore no Flibe-water reaction needs to be considered. However, if a common cause failure (e.g., seismic) causes a water-containing SSC and Flibe-containing SSC to fail concurrently, the amount of water that Flibe could be exposed to is assumed to be limited to an upper bound limit by design. When interacting with this upper bound amount of water, Flibe redox potential is still maintained within the bounds of salt chemistry conditions defined for the evaporation model; therefore, does not result in additional release of radionuclides from Flibe through evaporation.

3.4.2.8 Mass loss of structural graphite and pebble carbon matrix

Pebbles and structural graphite not submerged in Flibe can oxidize when exposed to air. If the mass loss of the pebble carbon matrix does not extend to the fueled zone, tritium release is the only additional MAR release pathway to be considered when fuel pebble oxidizes. Tritium is puff released from oxidized pebble carbon matrix and oxidized structural graphite. In the MHA analysis, the assumed temperature for pebble carbon matrix is so high that all available tritium is effectively puff-released from the pebble carbon matrix. The portion of structural graphite unsubmerged in Flibe is small. The inventory of tritium puff released (instead of as a function of temperature) from oxidization of structural graphite not submerged in Flibe is accommodated by the following inherent conservatism in the treatment of tritium in the MHA:

- Conservative inventory of tritium available for release
- Conservatively high assumed temperature of pebbles
- Moderator pebbles assumed to have the same temperature as fuel pebbles

3.4.2.9 Peak structural graphite temperature

Tritium is release from structural graphite as a function of temperature. During a postulated event, the peak structural graphite temperature is bounded by temperature-time curves derived from the assumed MHA structural graphite temperature-time curve to limit tritium release to the amount during the MHA. Bounding temperature-time curve derived from the assumed MHA temperature-time curve can be based on integrated effects on dose.

3.4.2.10 Peak pebble carbon matrix temperature

Tritium is released from pebble carbon matrix as a function of temperature. During a postulated event, the peak pebble carbon matrix temperature is bounded by temperature-time curves derived from the

© 2024 Kairos Power LLC

assumed MHA peak pebble carbon matrix temperature-time curve to limit tritium release to the amount during the MHA. Bounding temperature-time curve derived from the assumed MHA temperature-time curve can be based on integrated effects on dose.

3.4.2.11 Amount of materials at risk released

During a PHSS break, additional materials at risk can be released through graphite dust and mobilized Flibe in the system. As these are not release pathways in the MHA, the equivalent dose of these materials at risk released is limited to below a derived limit to ensure these release pathways do not cause the consequence of this postulated event to exceed those of the MHA.

© 2024 Kairos Power LLC

4 EVALUATION MODELS

4.1 SYSTEMS ANALYSIS

4.1.1 KP-SAM Code Description

The System Analysis Module code, also known as SAM, was developed by the U.S. Department of Energy and Argonne National Laboratory as a generic system-level safety analysis tool for advanced non-LWRs. The code solves tightly coupled physical phenomena including fission reaction, heat transfer, and fluid dynamics in reactor structures, systems, and components.

Kairos Power has developed and maintained a KP-FHR specific code based on SAM with the capabilities of SAM called KP-SAM.

KP-SAM is directly built on the Multiphysics Object Oriented Simulation Environment (MOOSE) framework at shown in Figure 4-1 which handles most of the numerical methods, output processing and most of the input processing. MOOSE and its base packages like LibMesh and PETSc are open-source software thus the major development from SAM to KP-SAM includes a description of the physics and system component behaviors, handling specific numerical methods such as continuous Finite Element Method stabilizing methods, and adding specific functions for the systems code.

KP-SAM, like SAM uses simplified thermal hydraulic models to represent the major physical components and describe major physical processes such as fluid flow and heat transfer. The main types of components in SAM are listed below.

- Basic geometric components describing individual 1-D/2-D fluid or solid domains
- 0-D components for setting boundary conditions for 1-D fluid domains
- 0-D components for connecting 1-D components
- Assembly components that are constituted by combining different basic geometric components or 0-D connecting components
- Non-geometric components for physics integration, control and trip systems, or special 1-D models such as the point kinetic model

4.1.1.1 Physical Models and Equations

KP-SAM, like SAM has two types of physics models: field equations and closure models. Field equations are solved to determine the transport of the quantities of interest in 0-D, 1-D, or 2-D domains. The single-phase flow field equations in KP-SAM shown in Equation 10 include 1-D mass, momentum, and energy conservations along the flow direction.

$$\frac{\partial \rho}{\partial t} + \frac{\partial (\rho u)}{\partial s} = 0$$

$$\rho \frac{\partial u}{\partial t} + \rho u \frac{\partial u}{\partial s} = -\frac{\partial p}{\partial s} + \rho g_s - \frac{f}{D_e} \frac{\rho u |u|}{2} \tag{10}$$

$$\rho c_p \frac{\partial T}{\partial t} + \rho c_p u \frac{\partial T}{\partial s} = \frac{q_s'' P_h}{A_c}$$

© 2024 Kairos Power LLC

$$\rho = \rho(p, T)$$

where,

ρ = coolant density

u = velocity

T = coolant temperature

t = time

s = the axial coordinate in flow direction

p = pressure

$g_s = g \cdot \cos\theta$

θ = angle between the flow direction and gravity vector

g = the gravity constant.

f = friction coefficient

D_e= equivalent hydraulic diameter

c_p = the specific heat

q_s'' = the convection heat flux from solid surface

P_h and A_c = heated perimeter and cross-sectional area of the coolant channel respectively.

The primary variables for the single-phase flow model in KP-SAM are the pressure, velocity, and temperature.

Heat structures model the heat conduction inside the solids and permit the modeling of heat transfer at the interfaces between solid and fluid components. Heat structures are represented by 1-D or 2-D heat conduction in Cartesian or cylindrical coordinates. One-dimensional spherical heat conduction model is also developed for pebble bed simulation. Temperature-dependent thermal conductivities and volumetric heat capacities can be provided in tabular or functional form from user-supplied data, or directly provided by the code and accessed through given material names. The modeling capabilities of heat structures can be used to predict the temperature distributions in solid components such as fuel pins or plates, heat exchanger tubes, and pipe and vessel walls, as well as to calculate the heat flux conditions for fluid components. The thermal conduction inside the solid structures is governed by the heat conduction equation.

KP-SAM includes a TRISO particle average temperature model associated with pebble bed core channel component model. The fuel pebble of KP-FHR design has a fuel annulus layer between the central low-density core and outer fuel-free shell. TRISO model in KP-SAM simulates temperatures of the fuel kernel, buffer, and cover (the IPyC, SiC, and OPyC lumped together), in addition to the average temperature in fuel annulus which is modeled by heat structure model.

Special 0-D models can be taken as 0-D field equations. The 3-D field equations are integrated over the domain and the partial differential equations become ordinary differential equations. The spatial integration process needs special spatial profile assumptions. The special 0-D models in KP-SAM include

© 2024 Kairos Power LLC

the volume branch, valve, pump, tank, point kinetic models, thermal radiation, and gap conductance models.

The widely used point kinetics equations model for multiple groups of delayed neutron precursors was implemented in KP-SAM with fully implicit time scheme options available up to 5th order accuracy. The decay heat power can be calculated from the user provided decay curve, or the ANSI/ANS-5.1-2005 standard method. Whichever method is used, uncertainty factors will be applied to ensure it is conservative. For the predictive decay heat model, the fissile material fission fractions include U-235, U-238, Pu-239, and Pu-241 and are provided by the reactor core design calculation. The fission ratios of fissile materials are provided for various stages of operation (build up). A sensitivity factor can also be applied to the decay heat fraction in order to conservatively account for uncertainties in decay heat.

Closure relations are correlations and equations that help to model the terms in the field equations by providing code capability to model and scale particular processes. Typical closure models include wall friction factor and form loss models for different flow geometries, convective heat transfer correlations for different heat transfer surfaces and pump performance curves. For example, the Kerntechnischer Ausschuss (KTA) correlation (Reference 27) was used for pebble bed pressure drop calculations in the sample transient KP-SAM analysis. Fluid and solid properties, including equations of state are also needed to close the field equations. The fluids to be simulated include Flibe, intermediate salt, water, simulant oil, air, and argon gas.

Table 4-1 summarizes the models and the field equations used by KP-SAM.

4.1.1.2 Control System Description

The SAM control system is used to perform the evaluation of algebraic and simple ordinary differential equations; the trip system is used to perform the evaluation of logical statements. The fundamental approximation made in the design of control/trip system is that the execution of control/trip system is de-coupled from the other parts of the hydraulic systems. The main execution of individual control/trip units is set at the end of each time step.

4.1.1.3 Numerical Methods

SAM uses a continuous finite element methods formulation for the spatial discretization of the 1-D or 2-D field equations. The detailed discretization for both time and space is managed by MOOSE, with the code formulated such that the numerical method orders are controlled through user inputs. For fluid models, a spatial stabilization method is required to suppress checkerboard type spatial oscillations that manifest when solving advection dominated problems using continuous finite element methods. The Stream Line-Upwind/Petrov-Galerkin and the Pressure-Stabilizing/Petrov-Galerkin scheme are implemented in SAM to resolve the numerical instability issues (Reference 10).

The physics in SAM is integrated into a single fully coupled nonlinear equation system. The discretized nonlinear equation system is solved using a pre-conditioned Jacobian Free Newton Krylov method. The combination of the Jacobian Free Newton Krylov nonlinear solver and high order numerical methods for both time and space enables the capability to minimize numerical errors.

4.1.1.4 Quality Assurance and Configuration Control

The software quality assurance plan is designed to provide a framework for solving computational engineering problems. The software quality assurance plan includes roles and responsibilities for the software developer, reviewer, tester, and user as well as documentation and software review requirements. The software quality assurance plan also describes configuration management, change

© 2024 Kairos Power LLC

control, audit requirements, software engineering methods, standards, practices, conventions, and metrics to be used, the control of support software, training and records that are to be collected, maintained, and retained.

4.1.2 KP-SAM Verification and Validation Plan

KP-SAM will be verified and validated prior to the final safety analysis.

The KP-SAM verification process confirms the software functions as designed (i.e., software verification); and that the equations are correctly solved by the code (i.e., numerical verification.) In a systems code, software verification is through regression tests covering the components, boundary conditions, functions for steady state, restart, etc.

The KP-SAM validation compares simulation results against experimental data. Unit test covers simple test data and is used to validate fluid and solid properties and heat transfer and wall friction correlations. Separate effects test validation covers the important thermal-hydraulic phenomena relevant during accident conditions, as identified by the PIRT. Integrated effects test validation covers scaled integral tests at system level or plant level, often at different scales to avoid scaling distortion. Reactor tests provide more direct evidence that the systems code can accurately simulate transient responses. The thermal-hydraulic and reactor physics strongly coupled unprotected events can only be performed with a test reactor.

The assessment of the KP-SAM EM adequacy includes the evaluation of closure relations and the integrated EM adequacy to quantify uncertainties.

4.1.3 Plant KP-SAM Model

A sample base KP-SAM model is provided for events that require a systems analysis. This base model can be modified according to the specific modeling needs for each event. It is provided here as an example of an acceptable model for use with the transient methodology.

The KP-SAM model includes upper and lower plena, a subdivided core based on flow area and correspondingly subdivided reflector, downcomer, vessel, and cooling panel sections. A set of primary piping is included in the model making up the hot and cold legs of the reactor and includes models for a pump and a IHX. Non-fuel/IHX heat structures in the model are 2D in order to model axial heat transfer. The reactor power is modeled using a point kinetics and decay heat model. The temperature profile within the pebble is modeled by a 1D conduction model with a special model for TRISO particles within the fuel layer of fuel pebbles.

A reflector bypass channel is modeled to capture the effect of flow from the lower plenum bypassing the core in favor of the flow path through the reflector. The area of this bypass channel is set such that an assumed conservative fraction of the flow makes its way directly from the lower plenum to the upper plenum. A bypass flow path containing a fluidic diode is also included in the model to redirect the coolant in the upper plenum down into the downcomer during natural circulation mode.

The IHX is utilized during steady state to reject heat from the system and control the lower plenum temperature. The secondary side of the IHX is defined by time dependent boundary conditions. Similarly, the DHRS is modeled by radiatively coupling vessel heat structures and cooling panel heat structures and placing a temperature boundary condition on the outside wall of the cooling panels. The instrumentation and control system is modeled by the KP-SAM trip and control system. The sample

© 2024 Kairos Power LLC

KP-SAM nodal diagram is depicted in Figure 4-2. Table 4-2 summarizes KP-SAM components used for each region in the sample nodal diagram.

A hot channel factor method conservatively envelopes the maximum bulk coolant temperature in the core for fuel performance analysis:

$$T_{flibe-hcf} = T_{flibe-lp} + \left(T_{flibe-max} - T_{flibe-lp}\right) * hcf_{flow} * hcf_{power} \quad (11)$$

where,

$T_{flibe-hcf}$ = conservative maximum coolant temperature

$T_{flibe-lp}$ = lower plenum coolant temperature

$T_{flibe-max}$ = calculated peak coolant temperature

hcf_{flow} = direct flow hot channel factor

hcf_{power} = direct power hot channel factor

In this highly simplified method, it is assumed that anything that could skew the reactor power profile or coolant distribution within the core happens in coincidence. The method is made further conservative by scaling the gradient between the KP-SAM calculated peak coolant temperature and the lower plenum temperature instead of taking the coolant temperature to be at the node with maximum fuel temperature.

The direct power hot channel factor (e.g., 1.3) accounts for radial peaking and uncertainties in the neutronic calculations. Power measurement uncertainty is handled explicitly by biasing the reactor power in the model. The direct flow hot channel factor (e.g., 1.2) and is intended to take into account any kind of bulk flow maldistribution from sources such as pump intake placement that could be present in the core. It is not necessary to derive a subfactor for flow bypassing the core and traveling through the reflector because this is modeled explicitly.

Once a reactor trip is initiated and the control and shutdown elements start to insert, the reactor power transient is mainly affected by the negative reactivity insertion by the control and shutdown elements insertion. The position dependent control and shutdown element worth is determined by nuclear core analysis and is applied in the safety analysis with added uncertainties. The most limiting minimum control system worth is used, considering the reactor core fuel cycle, which is assumed to be the equilibrium core. The element insertion speed is conservatively applied, as well.

4.2 FUEL PERFORMANCE

The code KP-BISON is used to model fuel performance using the methodology described in Reference 7. The evaluation model for postulated events uses KP-BISON with a conservative approach to assess the pre-transient fuel failure probability and radionuclide release during normal operation to inform the state of the fuel at event initiation. The modeling of the normal operation phase relies on two bounding trajectories (i.e., physical paths followed by the fuel pebbles in the core along which they accumulate burnup and fast fluence) to ensure conservative pre-transient fuel failure probabilities and fission product release fractions:

- A low-temperature trajectory is used to compute the probability of failure of the SiC layer by IPyC cracking.

- A high-temperature steady-state trajectory is used to compute the probability of pre-transient failure of the TRISO particle by over-pressure and of the SiC layer by chemical attack and the fractional release of radionuclides.

The two trajectories both follow the irradiation history that achieves discharge burnup and maximum fast fluence of the fuel and use the minimum cold leg inlet and maximum core hot channel outlet temperatures as baseline temperatures to calculate conservative isothermal pebble surface temperatures based on pebble-coolant heat transfer and potential local conditions (e.g., pebble-pebble contact, etc.). These isothermal temperatures are used to calculate the low and high fuel temperatures applied to the TRISO particles for the calculation of the pre-transient failure probabilities and radionuclide release fractions.

Modeling of the normal operation phase is included in the methodology because TRISO particles are more likely to fail during normal operation and in-service failures must be accounted for in addition to manufacturing defects. Additionally, radionuclides transported throughout the coating layers during the normal operation phase are, in general, more readily available to be released during transients.

The postulated events are modeled at the end of the normal operation phase to maximize the probability of pre-transient IPyC cracking, the fission gas inventory that builds up internal pressure, and the time-dependent palladium penetration. At the initiation of the events, in-service failures from the normal operation phase are added to manufacturing defects (Table 4-3). Incremental failures from the transient phase are then calculated by KP-BISON, using the power and temperature profiles of the transient.

The corresponding radionuclide release fractions are calculated for the various TRISO particle cohorts (e.g., intact, defective, or failed) and combined with the relative fractions of each of these cohorts to provide an overall radionuclide release from the fuel.

The TRISO fuel pre-transient failure modes can lead to five different mechanical states for the TRISO particles:

- Intact
- Cracked IPyC
- Cracked IPyC + failed SiC (from IPyC cracking leading to SiC failure)
- Failed SiC (from Pd penetration)
- Failed TRISO (all coating layers failed from internal overpressure)

In addition, TRISO particles can have defective layers from manufacturing. Five compromised states result from particles being either defective or failed. Intact particles add a sixth possible state. These six states are each associated with a probability of occurrence:

- Intact $(1 - d_I - d_S - d_O - d_T) \times (1 - f_I - f_{IS} - f_S - f_T)$
- Compromised IPyC $d_I + (1 - d_I - d_S - d_O - d_T) \times f_I$
- Compromised IPyC + SiC $(1 - d_I - d_S - d_O - d_T) \times f_{IS}$
- Compromised SiC $d_S + (1 - d_I - d_S - d_O - d_T) \times f_S$
- Compromised OPyC d_O

© 2024 Kairos Power LLC

- Compromised TRISO $d_T + (1 - d_I - d_S - d_O - d_T) \times f_T$

Where d_I, d_S, d_O, and d_T are the defective fractions of the IPyC layer, SiC layer, OPyC layer, and TRISO particle (i.e., exposed kernel), respectively, while f_I (cracked IPyC), f_{IS} (cracked IPyC + failed SiC), f_S (failed SiC), and f_T (failed TRISO) are the in-service failure fractions for the TRISO fuel failure modes.

Radionuclide release is calculated for each of the intact and five compromised states and the overall radionuclide release from the population of TRISO particles is obtained by weighting the resulting release fractions by the probabilities of occurrence of these states. Dispersed uranium is assumed to be fully released from the TRISO particles and its contribution is added to the release from the intact and compromised particles.

The verification and validation plans for the KP-BISON code are summarized in Reference 7.

4.3 NEUTRONICS

The Serpent2 code is used for neutronics calculations. The Star-CCM+ code is used for both discrete element modeling of the pebble flow and porous media approximation for thermal-hydraulics feedback. The description of these tools and models along with validation, verification, and uncertainties are presented in Reference 8.

4.4 STRUCTURAL ANALYSIS

The materials qualification plan for high temperature metallic materials is provided in Reference 9. The materials qualification plan for graphite materials is provided in Reference 11. These qualification plans inform the figures of merit for the reactor vessel and internals described in this report. The structural analysis of the materials under postulated event conditions will be performed prior to submittal of an Operating License Application.

4.5 EVENT-SPECIFIC METHODS

This section provides the event-specific methods that use the evaluation models with conservative inputs to analyze the transients discussed in Section 3. Key model uncertainties and initial conditions are conservatively applied to the methods to ensure figures of merit are conservatively predicted. Parameter ranges considered for all events are provided in Table 4-4. Sample results for the postulated event categories are provided in Appendix A to illustrate the transient methodologies.

4.5.1 Salt Spills

The salt spill event category is described in Section 3.2.2. The analysis of the bounding salt spill event is composed of the following models:

- Single phase break flow model – the mass flow rate with time through the break and the final upper plenum free surface level are the two major modeling results. Two-phase flow due to gas entrainment is prevented through the primary pump design. Two modeling options are available: (a) KP-SAM model based on the slight modification of the baseline plant model to include the single-phase break flow model; and (b) a conservative analytical model
- Long term performance of passive decay heat removal model – this is similar as the model used for loss of forced circulation overheating bounding case but with reduced free surface level.
- Radioactive source term release models to estimate the bounding total release from the event. Two major source term models are required:

© 2024 Kairos Power LLC

- Aerosol generation rate and amount due to single phase coolant jet.
- Fission product evaporation rates and amount from the spilled Flibe pool and from the in-vessel Flibe free surface.

- Air ingression and graphite oxidation models – general gas flow model is available in KP-SAM; a KP-SAM input model is used to perform the analysis:
  - General gas flow model including buoyancy driven counter current flow limits the oxygen concentration in the cover gas space.
  - Graphite oxidation model provides bounding graphite density reduction rate.
  - A special KP-SAM input model will capture the major components involving air ingression and graphite oxidation models.
- Acceptance criteria – the third method discussed in Section 3.4, using both direct dose calculation for some release pathways and figures of merit for other pathways, is used to demonstrate that this postulated event is bounded by the MHA.

4.5.1.1 Initial Conditions

The initial conditions for the limiting scenario must be provided and justified. The limiting scenario is assumed to occur when the reactor is operating at full power and operating pressure and has been operating long enough for the fuel to contain fission products at equilibrium concentrations. Therefore, the maximum possible decay heat is available at the start of the event. Although the hypothetical double-ended guillotine hot leg break at the IHX inlet is considered the bounding case, the entire spectrum of break sizes and location must be considered to confirm that the double-ended guillotine break is bounding.

The initial conditions for the amount and distribution of MAR immediately before the break must be determined to calculate a source term for this event. As this event does not involve the PHSS, the MAR in PHSS is excluded from the analysis. The initial MAR distribution is summarized below:

Fuel Pebble MAR

The majority of the MAR is contained by the TRISO particles in the fuel pebbles in the core. The inventory of MAR in the fuel is established through code analysis using Serpent2. The defect ratio of TRISO particles, the additional in-service failure of the particles, and the fraction of heavy metal contamination are specified through fuel qualification requirements (Reference 12).

Flibe in MAR in the Primary System

A conservative amount of MAR in the Flibe is assumed in the circulating activity in the coolant. Note there may exist small amount of graphite dust which is suspended within the Flibe. The dust behaves as getter and absorber of tritium. The chemistry control system ensures the loading of graphite dust is within acceptable bounds.

© 2024 Kairos Power LLC

Graphite and Metal Structures MAR

Only tritium is considered to be absorbed by graphite and metal structures based on existing knowledge. The amount of tritium in graphite and metal structure is estimated with the same conservative approach as in the MHA.

Cover Gas MAR

A conservative amount of MAR in the argon cover gas is assumed to account for the activity of the cover gas system.

4.5.1.2 Transient Analysis Methods

Volume of Spilled Flibe

To evaluate release of MAR to the building air space and eventually to the environment air, the amount of Flibe that can be spilled is determined. A coolant level trip signal from the reactor protection system is credited to trip the pump. Once the pump is tripped, it coasts down until the pump flow rate drops to almost zero. At this point, a vacuum breaker is activated to allow air to enter the high point of the hot leg preventing syphoning the Flibe in the vessel. Another similar vacuum break located in the cold leg also allows air to enter the high point of the cold leg too. The volume of the Flibe that is spilled out of the break is evaluated as:

$$V_{spill} = V_{CL} + V_{HL} + V_{coast} \tag{12}$$

where V_{CL} is the volume of Flibe in the cold leg between the elevation of cold leg nozzle and the elevation of the break, V_{HL} is the total volume of the Flibe in the hot leg, and V_{coast} is the accumulative volume pumped out from the time of pump trip to the fully coast-down condition. Assume the pump volumetric flow follows a coast-down curve given by

$$\dot{V(t)} = \dot{V}_0 e^{-\frac{t}{t_{coast}}} \tag{13}$$

where $\dot{V}(t)$ and $\dot{V}_0$ are pump volumetric flow and the flow at normal operation, t_{coast} is a characteristic pump coast down time, equals $t_{1/2}/\ln(2)$, where $t_{1/2}$ is the time when the pump volumetric flow is reduced by half. The total volume pumped out during the coast down time is then given by

$$V_{coast} = \dot{V}_0 t_{coast} = \frac{\dot{V}_0 t_{1/2}}{ln(2)} \tag{14}$$

Therefore, for given value of $t_{1/2}$ and hot leg and vessel geometries, the volume of the spilled Flibe can be determined through Equation 12. Note: Equation 12 assumes that V_{coast} is less than the volume from the low-low set point level to the pump suction. If the cumulative volume is larger than the volume V_{psp} from the low-low set point level to the pump suction level, V_{psp} should be used to replace V_{coast} in Equation 12, because in this condition the pump suction is exposed before the pump fully coasts down.

The methods to evaluate the releases from the fuel pebbles, remaining Flibe, graphite and metal structures in the vessel is identical to that of MHA, with the following exceptions:

© 2024 Kairos Power LLC

- The concentrations of MAR remaining in the vessel are given by circulating activity alone, while the concentration in MHA is the sum of the circulating activity and the concentrations due to additional fuel release assumed in MHA event.
- Temperatures of Flibe, fuel and structures in this event are evaluated with KP-SAM based on conservative assumptions of decay heat removal capabilities and other boundary conditions, while the temperatures in MHA event follow a bounding temperature versus time curve.

Instantaneous Release from Spilled Flibe

The instantaneous release is the phase right after the break, when the discharged Flibe forms a jet. The release is dominated by two mechanisms that generate aerosols: jet breakup, and splashing and spilling when Flibe falls onto the ground.

When Flibe is discharged from the vessel to the building, it forms a coherent jet before it breaks up into droplets. If the falling height from the break location to the ground is shorter than the breakup distance, the jet is not expected to break up and minimum amount of aerosol is generated. For conservatism, it is assumed the jet is always broken up no matter how short the falling height is. Most droplets from the jet break are too large to be considered as aerosol particles because they deposit quickly under the gravity. However, a small fraction of the droplets is small enough to be suspended in the air and transported as aerosols. To estimate this fraction of the aerosols, the Sauter Mean Diameter which is the average diameter based on the ratio of total volume and total surface area, is evaluated first through an equation by Epstein (Reference 13) which is based on an even earlier derivation by Mayer (Reference 14):

$$SMD = \frac{36.4}{C_D^{\frac{4}{3}}}\left(\frac{\mu_f^2 \sigma \rho_f}{\rho_g^2 \Delta P^2}\right)^{\frac{1}{3}} \quad (15)$$

where C_D is loss coefficient of the break and ΔP is the pressure difference between the vessel and the building air. Assume the droplets follow a Rosin-Rammler size distribution (Reference 15) and the fraction of aerosol particles can be obtained through the cumulative fraction of the size distribution below a maximum diameter of $50\ \mu m$ (Reference 16). The maximum diameter is chosen to be consistent with the aerosol model in MELCOR code. The mass of aerosol generated through the jet break is then obtained from the product of total spilled mass of Flibe and the fraction of aerosols.

Aerosols can also be generated when the jet or droplets from the broken jet fall into a Flibe pool accumulated on the ground of reactor cell. When the jet hits the surface of the Flibe pool, it entrains air with it and forms bubbles in a layer adjacent to the surface of the Flibe. Bubble bursting produces very fine aerosol particles. The amount of air entrained by the jet and droplets is based on an empirical expression developed by Bin (Reference 17) as

$$\frac{Q_g}{Q_f} = 0.04 Fr_j^{0.28}\left(\frac{H}{d_0}\right)^{0.4} \quad (16)$$

where Q_g and Q_f are volumetric flow rates of the entrained air and Flibe flow, H is the falling height, and Fr_j is Froude number of the Flibe flow. Volumetric rate of aerosols generated through the bubble bursting is conservatively bounded by a linear expression (Reference 18)

© 2024 Kairos Power LLC

$$Q_{A,sp} = E \cdot Q_g \quad (17)$$

where E is an entrainment coefficient. A conservatively high value of E is 2.1E-6 (Reference 19). The aerosol generation due to the spilling and splashing is then obtained through the Flibe spilling rate and Equations 16 and 17.

MAR release associated with the aerosol generation is evaluated through the aerosol amount and the concentration of MAR in the spilled Flibe.

Evaporative Release from Spilled Flibe

The evaporative release is the phase when the discharge of the Flibe from the vessel ends and the spilled Flibe completes spreading on the reactor cell floor. Small amount of Flibe is likely to spread only a fraction of the reactor cell floor area before it is completely solidified. It is not a major concern for MAR release for partially spreading Flibe because it freezes quickly. More concern is large amount of spilled Flibe which spreads the entire area of the reactor cell floor. In this case, a Flibe pool is expected to form with a depth of molten Flibe. The bottom of the pool contacts with steel liner which is placed to prevent Flibe-concrete interaction. The top of the pool transfers heat to air through convection and to surrounding structures through radiation. No water and no water sources are present where the Flibe spreads, and Flibe-water interaction is excluded.

MAR release from the Flibe pool is dominated by evaporation over the top surface of the pool. It continues until the top surface is solidified. To evaluate the amount of MAR released, Flibe temperatures are evaluated first. The Flibe temperature is based on energy balance of the pool. For the downward heat transfer, a layer of solidified Flibe is expected between the liquid Flibe and the liner. A 1D moving boundary equation needs to be solved for the temperature profile within the solidified layer, and growth (or shrinkage) of the layer. The boundary condition at the interface between the liquid Flibe and the solidified layer is determined by Globe-Dropkin correlation (Reference 20). The boundary condition at the interface between the solidified layer and the underneath liner is given by gap conductance between the solidified layer and the liner, or through continuity conditions of temperature and heat flux if no gap is assumed. The heat transfer between the liquid Flibe to the top surface is determined by Globe-Dropkin correlation again, and the heat transfer on the air side is based on McAdams correlation (Reference 21) for natural convection and radiation with a low temperature heat structure. These heat transfer terms are combined to determine the energy change of the liquid Flibe due to heat transfer and solidification at the bottom, and eventually the temperatures of the liquid Flibe and at the top surface.

Once the temperatures are determined, evaporation rates are assessed with the same method as the MHA for MAR. The evaporation rate and integral release amount are evaluated until the temperature of the top surface is lower than the Flibe melting temperature.

4.5.2 Insertion of Excess Reactivity

The limiting insertion of excess reactivity is described in Section 3.2.2. The analysis of the limiting event in this category (a control element withdrawal) includes a systems analysis with conservative neutronics and fuel performance input.

© 2024 Kairos Power LLC

4.5.2.1 Initial Conditions

The initial conditions of the transient are biased to ensure a conservative evaluation of the figures of merit. The limiting control rod withdrawal scenario is assumed to initiate from the highest possible reactor power because the higher power provides the highest heat input to challenge the identified figures of merit. However, sensitivities must be performed to ensure that reactivity insertions from lower power levels do not unexpectedly challenge a figure of merit. A power uncertainty is applied to reactor power to bias the power high.

4.5.2.2 Transient Analysis Methods

The reactivity insertion transient involves a change in core reactivity that adds heat to primary system. Therefore, the event analysis requires information from the systems code, fuel performance, and neutronics EMs. The systems code, KP-SAM analyzes the event progression with inputs from the neutronics EM and provides inputs to the fuel performance EM.

The nuclear fission power profile within the pebble bed is affected by the neutron flux distribution in the core region and the fuel burn-up status of the pebbles. The current approach to modeling core power density is an axially resolved radially averaged method and does not explicitly account for radial power peaking in the core. The radial power profile and its effect on the coolant and fuel temperature are not explicitly modeled; therefore, local peak coolant and fuel temperatures are not fully resolved. The hot channel factor methodology described in Section 4.1 accounts for both power peaking and the possibility of flow being poorly distributed in the core.

In order to ensure a conservative evaluation of the limiting reactivity insertion event, the following conservatisms are applied to model inputs:

- Highest worth control element is assumed to be withdrawn.
    - The limiting reactivity insertion rate is determined from the limiting reactivity rod worth per length from neutronics EM, combined with the maximum control element withdrawal speed.
    - A range of reactivity insertion rates, up to and including the maximum reactivity insertion rate, are analyzed in the final safety analysis.
    - At full power and hot zero power, the initial control element position is assumed to be fully inserted in the reactor core.
    - A conservative treatment is applied to address the impact of a dynamic change in power shape associated with the control element movement.
- Least negative reactivity feedback coefficients are used to minimize the power suppression effect by the negative reactivity feedback in preliminary safety analysis.
- Most negative reactivity feedback coefficients are also be applied and analyzed to investigate the effect of delayed reactor trip in the final safety analysis.

This event is also identified as one of the bounding fuel performance cases and must be analyzed with the KP-BISON using the methodology described in Section 4.2.

4.5.3 Loss of Forced Circulation

The limiting loss of forced circulation scenario is described in Section 3.2.2. The analysis of the limiting event in this category includes a systems analysis with conservative neutronics input.

© 2024 Kairos Power LLC

4.5.3.1 Initial Conditions

The initial conditions of the transient are biased to ensure a conservative evaluation of the figures of merit. The limiting loss of forced circulation scenario is assumed to initiate from the highest possible reactor power because the higher power provides the highest heat input to challenge the identified figures of merit. However, sensitivities must be performed to ensure that loss of forced circulation events from lower power levels do not unexpectedly challenge a figure of merit.

4.5.3.2 Transient Analysis Methods

The important thermal and hydraulic phenomena during the transient include the flow friction (negative head) at the pump, heat transfer between the coolant and various interfacing structures such as pebble, reactor vessel wall and internals. Because the forced circulation is lost, the fluid friction through the coolant loop, including the reactor core, is more important than other events where forced flow is maintained.

KP-SAM is used to analyze the event progression with inputs from the neutronics EM and provides inputs to the structural integrity EM. Upon a loss of forced circulation, the reactor experiences an immediate increase in the fuel (pebble) temperature because of the reduced heat transfer to the coolant. The coolant temperature also rises because heat removal from the reactor core to the IHX is reduced and eventually stops. The increased temperature of the coolant could challenge the integrity of reactor vessel and core barrel structures.

The nuclear fission power profile within the pebble bed is affected by the neutron flux distribution in the core region and the fuel burn-up status of the pebbles. The current approach to modeling core power density is an axially resolved radially averaged method and does not explicitly account for radial power peaking in the core. The radial power profile and its effect on the coolant and fuel temperatures are not explicitly modeled; therefore, local peak coolant and fuel temperatures are not fully resolved. The hot channel factor methodology described in Section 4.1 accounts for both power peaking and the possibility of flow being poorly distributed in the core.

The KP-SAM base model described in Section 4.1 is used to analyze a loss of forced circulation event with the following modifications:

- Typically, the interaction between the fluid system and pump, during the transient, is modeled using head and torque curves of the pump. For the loss of forced circulation analysis, the coolant flow response is modeled without the detailed pump characteristics, by conservatively assuming the pump head after the transient starts. Since the pump rotor is assumed to stop instantly, the pump torque information is not needed.
- The reactivity feedback effect on power is minimized for conservative calculation by using least negative reactivity coefficient values to minimize the effect of power reduction from the initial temperature increase by the reduced coolant flow.
- The uncertainties in material properties of the Flibe coolant and vessel structures are addressed conservatively. The thermal mass of the material is reduced such that the temperatures of fuel and vessel structure are predicted higher. The reactivity feedback effect is modeled in such a way that the increased temperatures of the fuel, coolant, and structure (graphite) do not overestimate the negative feedback effect.

© 2024 Kairos Power LLC

- Reactor protection system setpoint and time delay: Reactor protection system signals initiate the reactor shutdown element to drop into the reactor core by a gravity. The setpoint detection and signal delay between the system are conservatively applied in the analysis.
- Head provided by the pump is reduced to zero on initiation of the event in order to model key aspects of pump seizure.

4.5.4 Pebble Handling and Storage System Malfunction

The limiting PHSS malfunction event is described in Section 3.2.2. The analysis of the limiting event in this category includes an event-specific evaluation model described in this section.

4.5.4.1 Initial Conditions

The initial conditions of the event are biased to ensure the maximum amount of MAR is released. The MAR in different barriers (regions) at the initial condition needs to be identified and quantified so that transient releases of MAR can be evaluated.

Fuel Pebble Spill During PHSS Transfer Line Break:

Due to the continuous refueling strategy used by the KP-FHR, fuel pebbles in the pebble transfer lines are either transported from the core to the PHSS or sent back to the core from the PHSS. As described in the event scenario in Section 3.2.2, it is assumed the longest transport line breaks causing pebbles to spill from the line. In addition, a delay time is assumed between the pebble spilling and the trip of the pebble extraction machine. The number of pebbles that can be spilled out of the break is based on three design parameters: the length of the transport line L, the speed of pebbles moving in the line u_{peb}, and the refueling rate u_{refuel}:

$$N_{spill} = \frac{L}{u_{peb}} + \Delta t_{delay} u_{refuel} \tag{18}$$

where Δt_{delay} in Equation 18 is the delay time. Conservatively, the spilled pebbles are assumed to have the highest burn-up and the largest amount of MAR among the pebbles.

Graphite Dust Accumulated in the PHSS:

The amount of graphite dust accumulated in the PHSS is based on an estimated maximum dust generation rate during normal operation. The concentration of MAR in the dust is assumed to be identical to the MAR in the graphite matrix of the pebbles with the highest burnup and loading of MAR. However, credit is taken for radionuclide decay during normal operation. For a radionuclide indexed by "*i*", the amount of the given radionuclide in the graphite dust is evaluated through the solution of the following equation:

$$\frac{dm_i}{dt} = \dot{m}_{dust} C_{0,i} - \lambda_i m_i \tag{19}$$

where, $\dot{m}_{dust}$ is the dust generation rate, $C_{0,i}$ is the concentration of the radionuclide in the graphite matrix, and λ_i is the decay constant of the radionuclide.

Flibe Accumulated in the PHSS:

A certain amount of Flibe is expected to be accumulated in the PHSS due to carrying over by pebbles. It is expected that the Flibe solidifies in the PHSS due to its low temperature compared to inside the reactor vessel. The MAR in the accumulated Flibe is based on the assumed conservative circulating activity of radionuclides in Flibe during normal operation.

Argon Gas in the PHSS:

It is assumed the amount of MAR in argon gas in the PHSS is small enough that it can be treated as de minimis for MAR release. The amount is bounded by the assumed conservative circulating activity of radionuclides in cover gas during normal operation.

Fuel Pebbles, Flibe, Graphite, Metal Structures, and Cover Gas in the Vessel

It is conservatively assumed that when the PHSS breaks, the vessel is not isolated and MAR in the vessel can be released through the break. The MAR in-vessel distributes in barriers including fuel pebbles in the core, Flibe, graphite and metallic structures, as well as cover gas. The amount of MAR is bounded by the MAR assumed in the salt spill event.

4.5.4.2 Transient Analysis Methods

The objective of the analysis of the PHSS break event is to evaluate key figures of merit for the event, so that the dose consequence can be assessed and demonstrated as being bounded by the consequence of the MHA.

The evaluation is performed with a combination of analyses using Serpent2 and KP-BISON. Serpent2 is used to calculate decay power and quantities of MAR, including tritium inventories in fuel and Flibe, and KP-BISON is used to calculate the amount of MAR held up in graphite and the initial MAR distribution in TRISO particles and the graphite matrix. The amount of tritium absorbed by fuel pebbles, graphite and metal structures is determined with the same approach as the MHA and is bounded for radionuclides in the Flibe and cover gas during normal operating conditions.

Upon determining the initial conditions of MAR as described above, quantitative analyses are made for barriers that are identified through the qualitative analysis process.

The number of fuel pebbles that can be spilled is obtained through Equation 18. The initial temperature, decay power and MAR concentrations in the graphite matrix are assumed to be conservatively high for the spilled pebbles.

When a pebble transfer line breaks, transporting pebbles for extraction or insertion, pebbles in the line can spill out of the break and fall on the floor of the building. The spilled pebbles, since the temperatures are high, can react with the air in the building to generate heat and transfer heat to the surrounding cool air through natural convection and thermal radiation. The heat removal rate through natural convection and radiation must be higher than the sum of decay heat and chemical reaction heat in order for the pebbles to be cooled and oxidation reduced to de minimis. However, before the pebble reaches a final stable condition, some mass of the pebble is lost due to oxidation and the MAR holdup associated with the lost mass released into the building air. The objective of the pebble oxidation model is to evaluate the fraction of the mass loss and MAR release until the pebble reaches a stable condition.

© 2024 Kairos Power LLC

Two major assumptions are made in the development of the pebble oxidation model:

- Each pebble can be considered separately from other pebbles for heat transfer and oxidation because pebbles are unlikely to pile up on the floor to form a pebble bed.
- The MAR released from a pebble is proportional to the mass loss of the pebble.

The oxidation of graphite is assumed to be in the regime I where oxygen infiltration occurs causing volumetric oxidation in the pebbles. The oxidation regime assumption is justifiable because of the transition temperature from the kinetics-controlled oxidation (regime I) to the kinetics and mass transfer-controlled oxidation (regime II). Test results on a graphite sample similar to the graphite used in the reactor indicate the transition temperature is as high as 700°C, but the highest temperature of spilled pebbles is less than 700°C.

For conservatism, the spilled pebbles are assumed to have the same decay heat, initial temperature, and MAR holdup concentration, which are set to conservatively high values to bound the consequence of pebble oxidation. The conduction equation of a sphere with internal heat generation is solved to obtain the temperature profile in a single pebble. Convective and radiation boundary conditions are assumed on the outer surface of the pebble, given by

$$-k\left.\frac{\partial T}{\partial r}\right|_{r=R} = -h\big(T(R) - T_g\big) - \epsilon\sigma(T(R)^4 - T_{hs}^4) \tag{20}$$

where T is pebble temperature, R is pebble radius, k is pebble thermal conductivity, h is the pebble's heat transfer coefficient, T_g is the gas temperature, ϵ and σ are the effective emissivity between two gray bodies and the Stefan-Boltzmann constant, T_{hs} is the temperature of the heat structure with radiation heat exchange with the pebble. The volumetric heat generation rate in the pebble is the sum of decay heat and the chemical reaction heat rates,

$$q''' = q'''_{decay} + q'''_{oxi} \tag{21}$$

and the volumetric oxidation heat generation rate is evaluated based on mass rate of oxidation as:

$$q'''_{oxi} = -\dot{m}_{oxi}\rho_C \Delta H_{oxi} \tag{22}$$

where $\dot{m}_{oxi}$ is the mass oxidation rate in units of $\frac{1}{s}$, ρ_C is the graphite density in unit of $\frac{kg}{m^3}$, and ΔH_{oxi} is the enthalpy change of oxidation reaction in units of J/kg. Note the negative sign in the equation of $q"_{oxi}$ is because a negative value of ΔH_{oxi} indicates an exothermal reaction. For conservatism, the highest enthalpy change of 32.792 MJ/kg (Reference 22) among all oxidation reactions between carbon and oxygen is used, which is the change for the reaction generating carbon dioxide. The oxidation rate is a function of temperature in the pebble. The oxidation rate correlations vary in literature because the types of graphite and properties are different. Here, the correlation by Zhou et. al. (Reference 28) for regime I oxidation is proposed for the analysis because the graphite sample in this literature is similar to the type of graphite that is used for pebbles of the reactor.

$$\dot{m}_{oxi} = 0.7194 \times 10^6 e^{-22362.13/T} \tag{23}$$

© 2024 Kairos Power LLC

where, the unit of the temperature T is Kelvin and the unit of the oxidation rate is 1/s. Solution of the energy equation leads to time dependent temperature and oxidation rate. The total mass loss of the graphite is obtained through the integral of the oxidation rate:

$$m_{oxi} = 4\pi\rho_C \int_0^t \int_0^R \dot{m}_{oxi}(r,\tau) r^2 dr d\tau \quad (24)$$

An estimate of the release of MAR which is originally held up in the graphite matrix of the spilled pebbles can be made according to the mass loss. The activities of hold-up MAR in the graphite matrix are estimated based on release of MAR from defective TRISO particles in the pebble, including those with defective SiC layers, exposed kernels, and heavy metal contamination. Such an estimate is conservative because it does not credit retention of radioisotopes by the defective particles, but instead assumes all the MAR in these particles are released and held by the graphite matrix in the pebble. By using this assumption, the activities of MAR in the graphite matrix are given by

$$A_{i,matrix} = A_{i,pebble} f_{defect} \quad (25)$$

where, subscript *i* is the index of the radioisotope of MAR, $\mathrm{A_{i,}}_{pebble}$ is the activity of the isotope in the pebble, and $\mathrm{f_{defect}}$ is the fraction of the defective particles including those with defective SiC layers, exposed kernels, and heavy metal contamination. The MAR is assumed to be uniformly distributed in the graphite matrix due to the large diffusion coefficient. Since the released MAR is assumed to be proportional to the mass loss of the pebble, the released MAR activities can be evaluated as

$$A_{i,rel} = N_{spill} A_{i,matrix} \frac{m_{oxi}}{m_{matrix}} \quad (26)$$

where subscript *i* is the index of the radioisotope of MAR, N_{spill} is the number of spilled pebbles, and m_{matrix} is the mass of the graphite matrix in a pebble.

Graphite Dust Accumulated in the PHSS:

Graphite dust is generated and accumulated in PHSS during normal operation due to pebble wear. Dust particles can behave like getters for MAR. When the PHSS breaks, the dust can be resuspended and expelled from the PHSS to building by the leakage gas flow resulting in an increase in radioactivity in the building gas space. The objective of the graphite dust resuspension model is to assess the amount of the resuspended dust and estimate the MAR releases due to resuspension.

The dust generation rate is determined in order to estimate the mass and activities of dust in the PHSS. The rate is based on an upper bound estimate of the specific wear rate of pebbles sliding on the surface of stainless-steel. The specific wear rate, w_{wear} in units of $\frac{kg}{N*m}$, is the rate of mass loss of pebbles due to wearing under unit normal force and sliding distance. For PHSS, the normal force of a pebble is the weight of the pebble, assuming there is no other mechanical force exerted on it during the pebble transfer and inspection. An upper bound sliding distance L_{slide} can be estimated since the detailed design of PHSS has not been completed. The mass generation rate is then given by:

$$\dot{m}_{dust} = w_{wear} L_{sliding} m_{pebble} g \cdot u_{refuel} \quad (27)$$

© 2024 Kairos Power LLC

where m_{pebble} is the mass of the pebble, g is the gravity acceleration rate, and u_{refuel}, is the number of pebbles extracted per second in units of $\frac{1}{s}$.

A major assumption of the graphite dust resuspension model is that the MAR concentration in the graphite dust equals the concentration in the graphite matrix where the dust is generated. However, credit is taken for decaying of radionuclides during normal operation. The assumption is conservative because the MAR concentration in graphite matrix has been estimated conservatively, as described above. Based on this assumption, the activities of MAR in the graphite dust can be determined through the following equation:

$$\frac{dA_{i,dust}}{dt} = \left(\frac{\dot{m}_{dust}}{m_{matrix}} A_{i,matrix} \cdot f_{pebble}\right) - \lambda_i A_{i,dust} \qquad (28)$$

where m_{matrix} and $A_{i,matrix}$ are mass of graphite matrix in a pebble, and the activity of the radioisotope in the matrix, and λ_i is the decay constant. f_{pebble} in the equation represents the fraction of the fuel pebbles in the core region, because there are a large number of graphite pebbles in the core that moderate neutrons. Therefore, a pebble that is extracted from the core region has a probability less than one being the fuel pebble, and only the dust generated by fuel pebbles contributes to the activity of MAR in the graphite dust. Solution of Equation 28 leads to a formulation of the activity of dust as the function of operating time t_{op} of the reactor:

$$A_{i,dust} = \left(\frac{\dot{m}_{dust}}{m_{matrix}} A_{i,matrix} \cdot f_{pebble}\right) \cdot \frac{1 - e^{-\lambda_i t_{op}}}{\lambda_i} \qquad (29)$$

The resuspension model in MELCOR (Reference 23) is used for the dust resuspension evaluation and assumes instantaneous resuspension based on the highest leakage gas velocity. The model was derived through the consideration of balance between the aerodynamic lift force and the adherence force. It evaluates a cut-off diameter of the resuspended dust particles, above which all the dust particles originally deposited on the surface of the structures are resuspended. The cut-off diameter is a function of the roughness, in microns, and the shear stress τ_w exerted by the gas flow given by

$$\tau_w = \frac{1}{2} C_f \rho_g u_g^2 \qquad (30)$$

where, C_f is the Fanning friction factor, ρ_g is the gas density and u_g is the gas velocity. The gas velocity can be determined through an expression (Reference 24) for compressible isentropic flow driven by pressure difference.

If the cut-off diameter is greater than or equal to 50 μm, the resuspended dust particles are not considered aerosols because the size is too large for airborne particles, i.e., the particles are expected to be deposited quickly once released from the PHSS. Otherwise, the fractional release of the graphite dust is evaluated with an assumed size distribution of dust particles. A log-normal distribution of the deposited particles is assumed by Friedlander (Reference 25) and the distribution was later used by MELCOR for comparison with the STORM experiment showing reasonable agreement.

© 2024 Kairos Power LLC

$$\phi(x) = \frac{1}{x\sigma\sqrt{2\pi}} exp\left(-\frac{(ln\, x - \mu)^2}{2\sigma^2}\right) \quad (31)$$

where, x is the particle diameter, $\phi(x)$ is the distribution function of particle number densities (i.e., $\phi(x)dx$ is the fraction of the number of particles with diameter x), $\mu = \ln(d_g)$ is the mean of the log-normal distribution, d_g is the geometric mean diameter, $\sigma = \ln(\sigma_g)$ is the standard deviation of the distribution, and σ_g is the geometric standard deviation. For the log-normal distribution, the geometric mean diameter and standard deviations of the deposited dust particles need to be provided as input. The resuspended fraction F_{lift} of the dust particles is determined as the fraction of the dust particles with diameters larger than the cut-off diameter but smaller than the upper limit diameter of aerosol particles $d_{aer} = 50\ \mu m$, i.e.,

$$F_{lift} = \frac{\int_{d_{crit}}^{d_{aer}} \phi(x) x^3 dx}{\phi_3} \quad (32)$$

where, d_{crit} is the cut-off lift diameter, $d_{aer} = 50 \mu m$ is the upper limit of the aerosol particles, and ϕ_3 is the third moment of the number distribution. Inserting the log-normal distribution of Equation 31 into Equation 32 results in an analytical formulation of the resuspension mass fraction:

$$F_{lift} = \frac{erf\left(\frac{ln\, d_{aer} - \mu'}{\sigma\sqrt{2}}\right) - erf\left(\frac{ln\, d_{crit} - \mu'}{\sigma\sqrt{2}}\right)}{2} \quad (33)$$

where, erf is error function, and $\mu' = \mu + 3\sigma^2$. The MAR in the resuspended dust particles is assumed to be released as aerosols promptly for conservativism.

© 2024 Kairos Power LLC

5 CONCLUSIONS

This postulated events and transient methodology described in this report meet the objectives described in NUREG 1537 (except for the rejection of potential events, which must be described in the Preliminary Safety Analysis Report). A comprehensive list of event categories is described to ensure that enough events have been considered to include any event that could result in significant radiological consequences. The initiating events and scenarios are categorized by type and a limiting case for each category is described. Consistent and specific acceptance criteria for the consequences of each postulated event are provided.

The methods described in this report are used to evaluate events within the design basis to ensure there are sufficient design features available to mitigate the effects and keep the potential consequences bounded by the MHA described in this report.

© 2024 Kairos Power LLC

6 REFERENCES

1. University of California Berkeley Nuclear Engineering. 2015. *Fluoride Salt Cooled High Temperature Reactor*. [ONLINE] Available at: http://fhr.nuc.berkeley.edu. (Accessed July 9, 2021).
2. Kairos Power, LLC, *Design Overview of Kairos Power Fluoride Salt Cooled, High Temperature Reactor.* KP-TR-001, Revision 1. February 2020.
3. Kairos Power, LLC, *KP-FHR Mechanistic Source Term Methodology Topical Report*. KP-TR-012-P-A. May 2022.
4. "MELCOR Fission Product Release Model for HTGRs," SAND2010-0800C Sandia National Laboratories, 2010.
5. B. J. Lewis, D. Evens, F. C. Iglesias, and Y. Liu, "Modelling of Short-Lived Fission Product Release Behavior During Annealing Conditions," Journal of Nuclear Materials, vol. 238, pp. 183–188, 1996.
6. "High Temperature Gas Cooled Reactor Fuels and Materials," International Atomic Energy Agency, Vienna, IAEA-TECDOC-1645, 2010.
7. Kairos Power, LLC, *KP-FHR Fuel Performance Methodology Topical Report*. KP-TR-010-P-A. May 2022.
8. Kairos Power, LLC, *Core Design and Analysis Methodology Technical Report*. KP-TR-017, Revision 1. September 2022.
9. Kairos Power, LLC, *Metallic Materials Qualification for the Kairos Power Fluoride Salt-Cooled High-Temperature Reactor Topical Report*. KP-TR-013-P-A. April 2023.
10. L. Cheng, A. Hanson, D. Diamond, J. Xu, J. Carew, D. Rorer, *Physics and Safety Analysis for the NIST Research Reactor*, BNL-NIST-0803, Rev. 1, March 2004.
11. Kairos Power, LLC, *Graphite Material Qualification for the Kairos Power Fluoride Salt-Cooled High-Temperature Reactor Topical Report.* KP-TR-014-P-A. April 2023.
12. Kairos Power, LLC, *Fuel Qualification Methodology Topical Report*. KP-TR-011-P-A. March 2023.
13. M. Epstein, *Flibe Aerosol Source Terms: Modeling Recommendations*. Memo of Fauske & Associates, October 23, 2019.
14. E. Mayer, *Theory of Liquid Atomization in High Velocity Gas Streams, ARS Journal* 31, pp. 1783-1785, 1961.
15. A.H. Lefebvre, and V. G. McDonell, "Atomization and Sprays, 2nd Edition," CRC Press, 2017.
16. "MELCOR Computer Code Manuals Vol. 1: Primer and Users' Guide Version 2.2.9541 2017, Section 3.1.5," SAND2017-0455 O, Sandia National Laboratories, January 2017.
17. A.K. Bin, "Gas Entrainment by Plunging Liquid Jets," Chemical Engineering Science, Vol. 48, No. 21, pp. 3585~3630, 1993.
18. T. Ginsberg, "Aerosol generation by liquid breakup resulting from sparging of molten pools of corium by gases released during core/concrete interactions," Nuclear Science and Engineering, vol. 89, no. 1, pp. 36~48, 1985.
19. M. Epstein, and M. Plys, "Prediction of Aerosol Source Terms for Dose Site Facility Applications," Proceedings of EFCOG Safety Analysis Working Group, April-May 2006.

© 2024 Kairos Power LLC

20. S. Globe, and D. Dropkin, *Natural-Convection Heat Transfer in Liquids Confined by Two Horizontal Plates and Heated from Below*, J. Heat Transfer, Vol 81, No. 1, pp. 24-28, February 1959.
21. W. McAdams, *Heat Transmission, 3rd Edition*, McGraw-Hill, New York, p. 180, 1954.
22. K. Jafarpur, Yovanovich, M.M., *Laminar Free Convective Heat Transfer from Isothermal Spheres: a New Analytical Method*, Int. J. Heat Mass Transfer, Vol 35, No. 9, pp. 2195-2201, 1992.
23. M. F. Young, "Liftoff Model for MELCOR," SAND2015-6119, Sandia National Lab, 2015.
24. S. Levy, *Two-Phase Flow in Complex Systems,* 1st Edition, Wiley-Interscience, August 1999.
25. S.K. Friedlander, *Smoke, Dust, and Haze: Fundamentals of Aerosol Dynamics*, 2nd Ed., Oxford University Press, 2000.
26. Electric Power Research Institute, "Uranium Oxycarbide (UCO) Tristructural Isotropic (TRISO) Coated Particle Fuel Performance," Topical Report EPRI-AR(NP)-A, 3002019978, November 2020.
27. Geschäftsstelle des Kerntechnischen Ausschusses, Nuclear Safety Commission of Germany (KTA). Safety Standard "Loss of pressure through friction in pebble bed cores." KTA 3102.3 1987; Issue 3/81.
28. X. Zhou, et. al., "Oxidation Behavior of Matrix Graphite and Its Effect on Compressive Strength," Science and Technology of Nuclear Installations, Vol. 2017.

© 2024 Kairos Power LLC

Table 2-1: Prescriptive Maximum Hypothetical Accident Temperatures

Start Time (Days)	End Time (Days)	Duration (Days)	Flibe Free-Surface and Structural Graphite Temperatures (K)	Kernel, SiC, and PyC and Pebble Carbon Matrix Temperatures (K)
0.00	0.01	0.01	1,000	1,423
0.01	0.08	0.08	1,000	1,089
0.08	3.00	2.92	1,089	1,089
3.00	4.00	1.00	1,059	1,059
4.00	5.00	1.00	1,029	1,029
5.00	6.00	1.00	999	999
6.00	7.00	1.00	969	969
7.00	8.00	1.00	939	939
8.00	9.00	1.00	909	909
9.00	10.00	1.00	879	879
10.00	30.00	20.00	859	859

© 2024 Kairos Power LLC

Table 3-1: Analyzed Postulated Events and Applied Evaluation Models

Event	KP-SAM	KP-BISON	Non-software based Special EM
Salt Spills	Air ingress and graphite oxidation models along with long term passive cooling input model	Not used	Coolant leaking model; Single phase jet aerosol generation model; Spilled Flibe pool heat transfer model
Insertion of Excess Reactivity	Systems model; Point kinetics equations model	Used as one of the fuel performance bounding cases	N/A
Increase in Heat Removal	Not used	Not used	A simple model to show that the maximum equivalent reactivity insertion due to increase in heat removal can be bounded by the Insertion of Excess Reactivity event.
Loss of Forced Circulation	Systems models for both overheating and long-term overcooling bounding cases	The overheating case used as one of the fuel performance bounding cases	N/A
Pebble Handling and Storage System Malfunction - Break	Not used	Not used	Pebble heat transfer and oxidation model; graphite dust resuspension model; source term release model

© 2024 Kairos Power LLC

Table 3-2: Derived Figures of Merit and Acceptance Criteria for Postulated Events

Figure of Merit	Acceptance Criterion	Applicable Events
Peak TRISO temperature-time	Generally bounded by temperature-time curves derived from the assumed MHA fuel temperature-time curve	Salt Spills, Reactivity Insertion, Increase in Heat Removal, Loss of Forced Circulation, PHSS break, Seismic, IHX Tube Break
TRISO failure probability	Negligible TRISO fuel failure probability	Salt Spills, Reactivity Insertion, Increase in Heat Removal, Loss of Forced Circulation, PHSS break, IHX Tube Break
Peak Flibe-cover gas interfacial temperature	Generally bounded by temperature-time curves derived from the assumed MHA Flibe-cover gas interfacial temperature-time curve	Salt Spills, Reactivity Insertion, Increase in Heat Removal, Loss of Forced Circulation, PHSS break, IHX Tube Break
Peak vessel and core barrel temperatures	Bounded by both the maximum allowable temperature derived to limit excessive creep deformation and damage accumulation and by 750°C (highest vessel design temperature)	Salt Spills, Reactivity Insertion, Increase in Heat Removal, Loss of Forced Circulation, PHSS break, IHX Tube Break
Minimum reactor vessel inner surface temperature	Above Flibe melting temperature	Loss of Forced Circulation (overcooling)
Airborne release fraction of spilled/splashed Flibe	Below airborne release fraction limit derived to bound total releases of the postulated event to less than the MHA	Salt Spills, Seismic, IHX Tube Break
Volatile product formation from Flibe-air reaction	Negligible amount of additional volatile products formed	Salt Spills, PHSS break, IHX Tube Break
Volatile product formation from Flibe chemical reaction with water, concrete, and/or construction materials (e.g., insulation, steel)	Negligible amount of additional volatile products formed	Salt Spill
Mass loss of pebble carbon matrix due to oxidation	Mass loss does not extend into the fueled zone	Salt Spills, PHSS break
Mass loss of structural graphite due to oxidation	Bounded by the MHA release	Salt Spills, PHSS break
Peak structural graphite temperature-time	Generally bounded by temperature-time curves derived from the assumed MHA structural graphite temperature-time curve	Salt Spills, Reactivity Insertion, Increase in Heat Removal, Loss of Forced Circulation, PHSS break, IHX Tube Break

© 2024 Kairos Power LLC

Figure of Merit	Acceptance Criterion	Applicable Events
Peak pebble carbon matrix temperature-time	Generally bounded by temperature-time curves derived from the assumed MHA pebble carbon matrix temperature-time curve	Salt Spills, Reactivity Insertion, Increase in Heat Removal, Loss of Forced Circulation, PHSS break, IHX Tube Break
Peak TRISO temperature-time ex-vessel	Generally bounded by temperature-time curves derived from the assumed MHA fuel temperature-time curve	PHSS break
Amount of material at risk released	Less than limit derived to bound total releases of the postulated event to less than the MHA	PHSS break, Radioactive Release from Subsystem or Component

© 2024 Kairos Power LLC

Table 4-1: KP-SAM Models and Field Equations

Model Name	Field	Description	Dimension
Single-phase flow	Mass, momentum, and energy	1-D fluid flow with wall friction and heat transfer. The flow model is single phase (liquid or gas) with the primary variables being pressure, velocity, and temperature.	1-D
Heat conduction	Energy	Heat conduction model for plate, cylindrical, or spherical geometries with temperature as primary variable. Can be coupled to 0-D/1-D fluid volumes such as pipes. May couple to other surfaces by thermal radiation or gap conductance model.	1-D/2-D

© 2024 Kairos Power LLC

Table 4-2: Sample KP-SAM Input Components by Nodal Type

Component Number	KP-SAM Type	Description
C01-C14	PebbleBedCoreChannel	Fueling (C01), Divergence (C02-C04), Active core cylinder portion (C05-C06), Convergence (C07-C12), Defueling (C13-C14)
F01-F10	PBOneDFluidComponent	Bypass (F01), Divergence (F02-F04), and Convergence (F05-F10) multi-pipes
T01	Tank	Pump bowls with free surface, cover gas, and vessel top head
F11	PBOneDFluidComponent	Primary pump draw line
P01	PBPump	Primary Salt Pump
F12-F13	PBOneDFluidComponent	Hot Leg Pipes
HX01	PBHeatExchanger	IHX
F14-F15	PBOneDFluidComponent	Cold Leg Pipes
F16-F17	PBOneDFluidComponent	Downcomer (split)
F18-30	PBOneDFluidComponent	Downcomer
E01	PBTDJ	IHX Secondary Inlet BC
E02	PBTDV	IHX Secondary Outlet BC
B01-B29	PBBranch	Junction connecting flow channels
VB01-VB02	PBVolumeBranch	Lower plenum (VB01), fluidic diode (VB02)
R01-R14, S01-S23	PBCoupledHeatStructure	Reflector structure (R01-R14), cooling panels (S01-S09), vessel (S10-S23)

© 2024 Kairos Power LLC

Table 4-3: KP-FHR TRISO fuel specification for as-manufactured contamination and defect fractions

Property	Specified Fraction
Dispersed uranium fraction	$\leq 1.0\times10^{-5}$
Exposed kernel fraction	$\leq 5.0\times10^{-5}$
Defective SiC coating fraction	$\leq 1.0\times10^{-4}$
Defective IPyC fraction	$\leq 1.0\times10^{-4}$
Defective OPyC fraction	$\leq 1.0\times10^{-2}$

© 2024 Kairos Power LLC

Table 4-4: Input Parameters Considered for Postulated Events

Parameter	Value	Rationale
Reactor initial power	Range of values up to and including maximum power level including uncertainty	Ranges of power levels analyzed
Coolant average temperature	Range over controller deadband and measurement uncertainty	Limiting value may be event dependent
System pressure	Nominal for all events except for salt spill	The effect of the system pressure is insignificant for all events except for salt spill events
Power distribution	Axial + radial power distribution for peaking factor Both fresh core and equilibrium core are considered as limiting conditions	Most limiting power distribution is considered
Shutdown margin	Considers most reactive shutdown rod is unavailable	Provide margin for malfunctions
Shutdown rod insertion time	Conservative shutdown rod insertion times assumed	Delays the shutdown of the reactor
Reactivity coefficients	Values assumed on an event specific basis and account for uncertainty	Limiting values may be event dependent
DHRS Capacity	Minimum and maximum performance assumed on an event specific basis Minimum performance assumes loss of a train of DHRS and minimum performance requirements Maximum performance assumes full capacity of DHRS plus uncertainty	Minimum DHRS performance is expected to be bounding for heatup events Maximum DHRS performance is expected to be bounding for overcooling events
Decay heat	Minimum and maximum values assumed on an event specific basis	Maximizing decay heat is expected to be bounding for heatup events Minimizing decay heat is expected to be bounding for overcooling events

© 2024 Kairos Power LLC

Parameter	Value	Rationale
Material properties	Ranged within uncertainties	Uncertainty in material properties for coolant and structures treated on an event specific basis
Reactor Protection System analytical limits	Actuation on: - High Reactor Power - High Flux Rate - High Coolant Temperature - Low Level	Analytical limits provide margin to safety limits Measurement uncertainty applied to setpoints are derived from analytical limits
Reactor Protection System actuation delay	Conservative delay times applied	Delay reactor trip
Plant Control Systems	Potential event mitigation capabilities of the plant control systems are not credited Suitably conservative treatment of relevant plant control features is applied in the safety analysis	Plant control systems are not safety related Potentially adverse performance of plant control systems needs to be considered

© 2024 Kairos Power LLC

Figure 1-1: Elements of Evaluation Model Development and Assessment Process

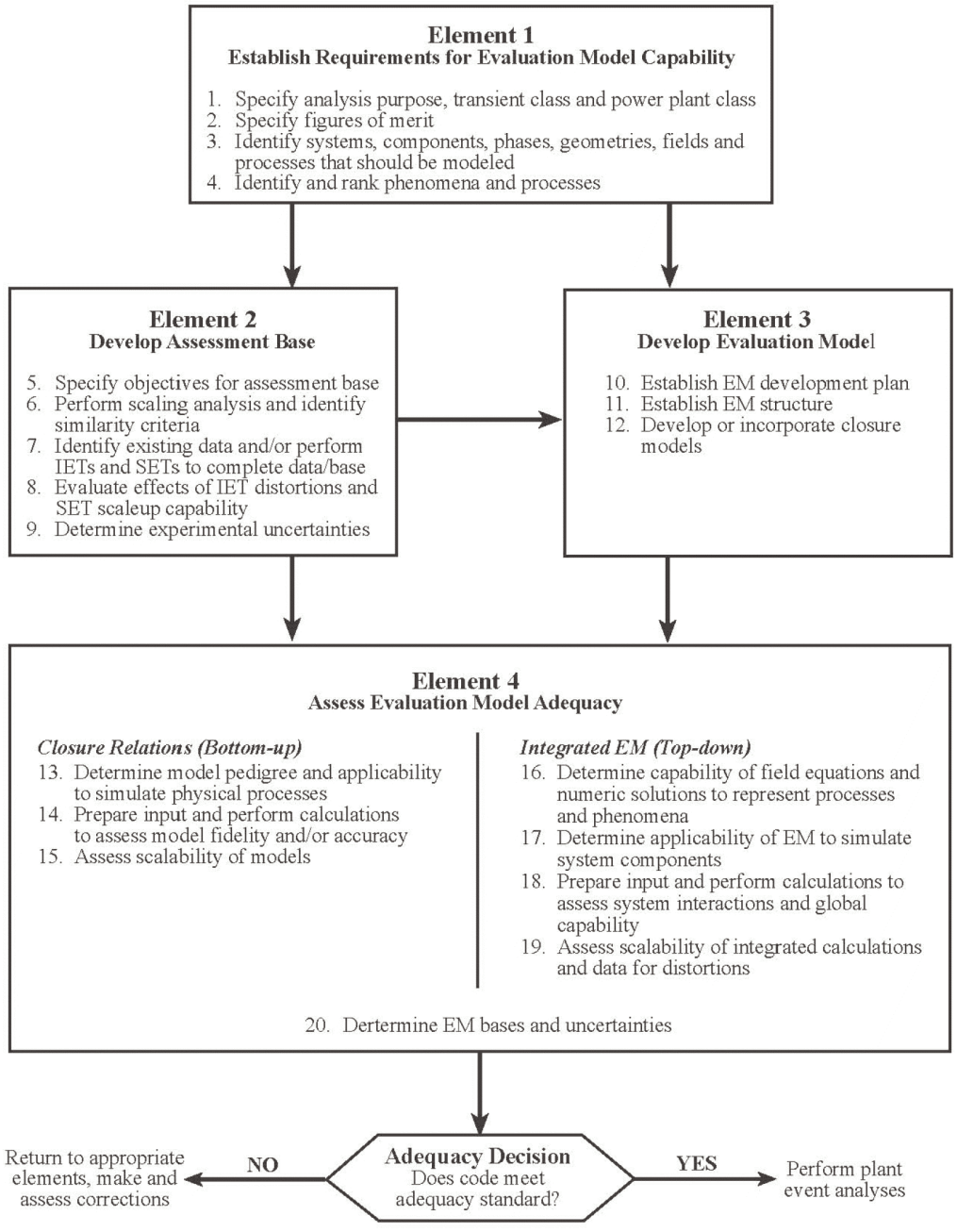

Figure 2-1: Prescriptive MHA Temperatures

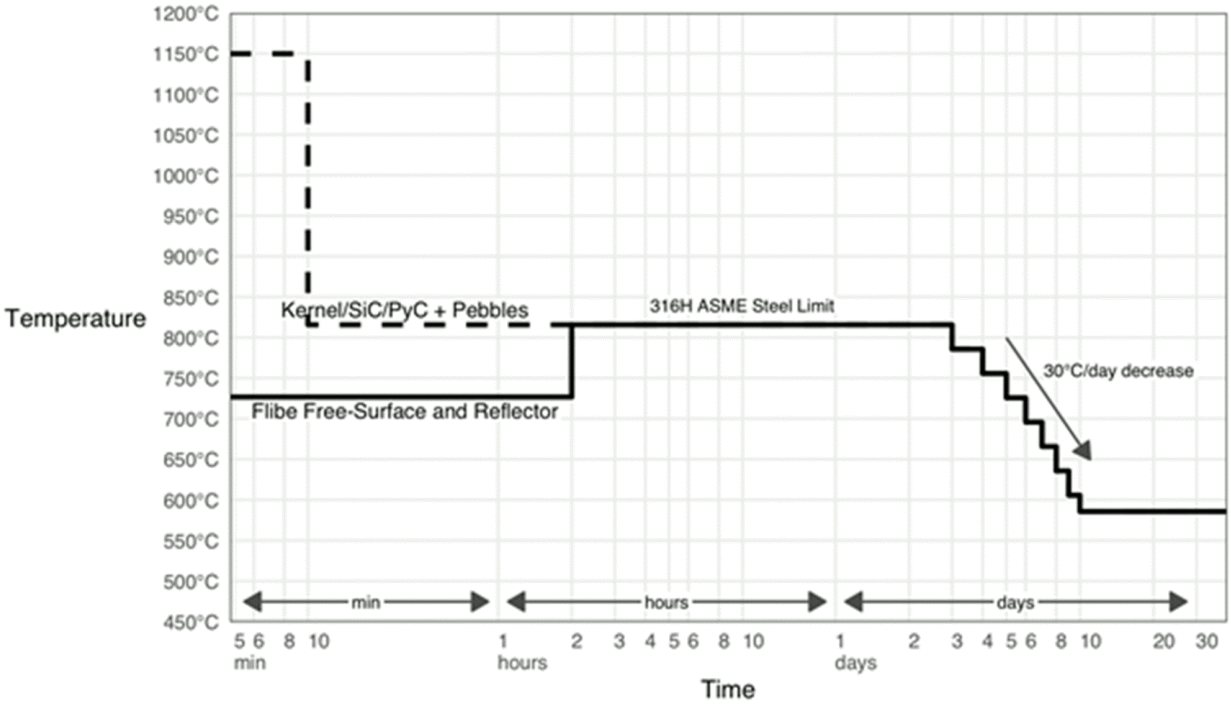

Figure 4-1: SAM Code Structure

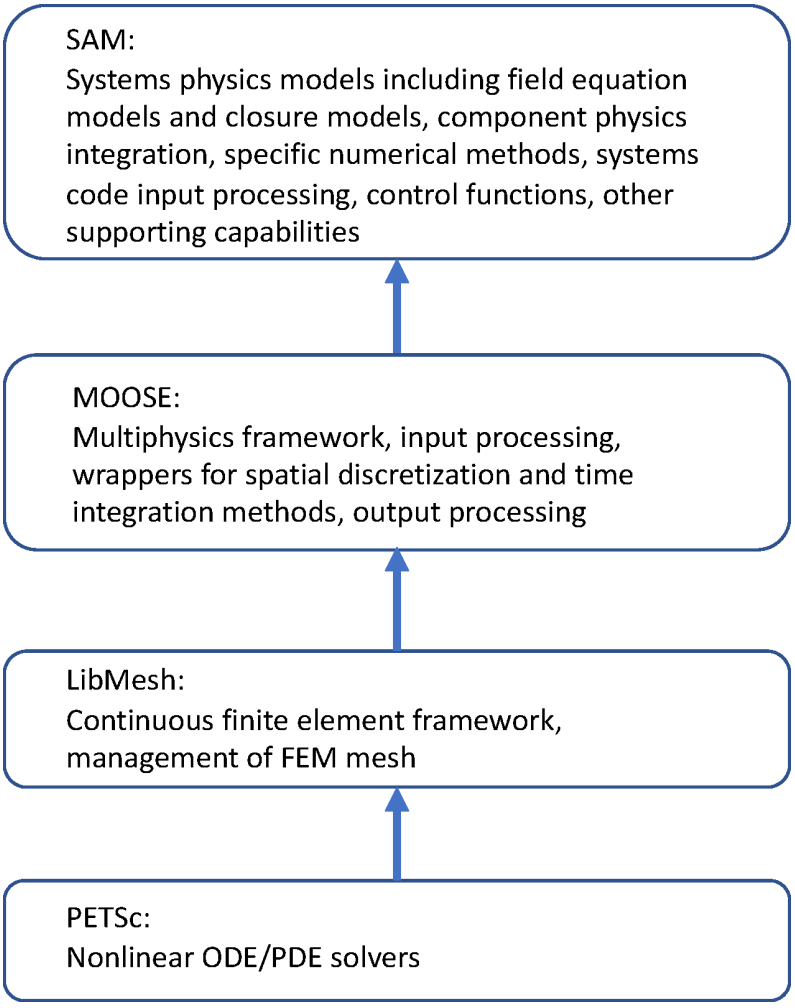

© 2024 Kairos Power LLC

Figure 4-2: KP-SAM Sample Nodal Diagram

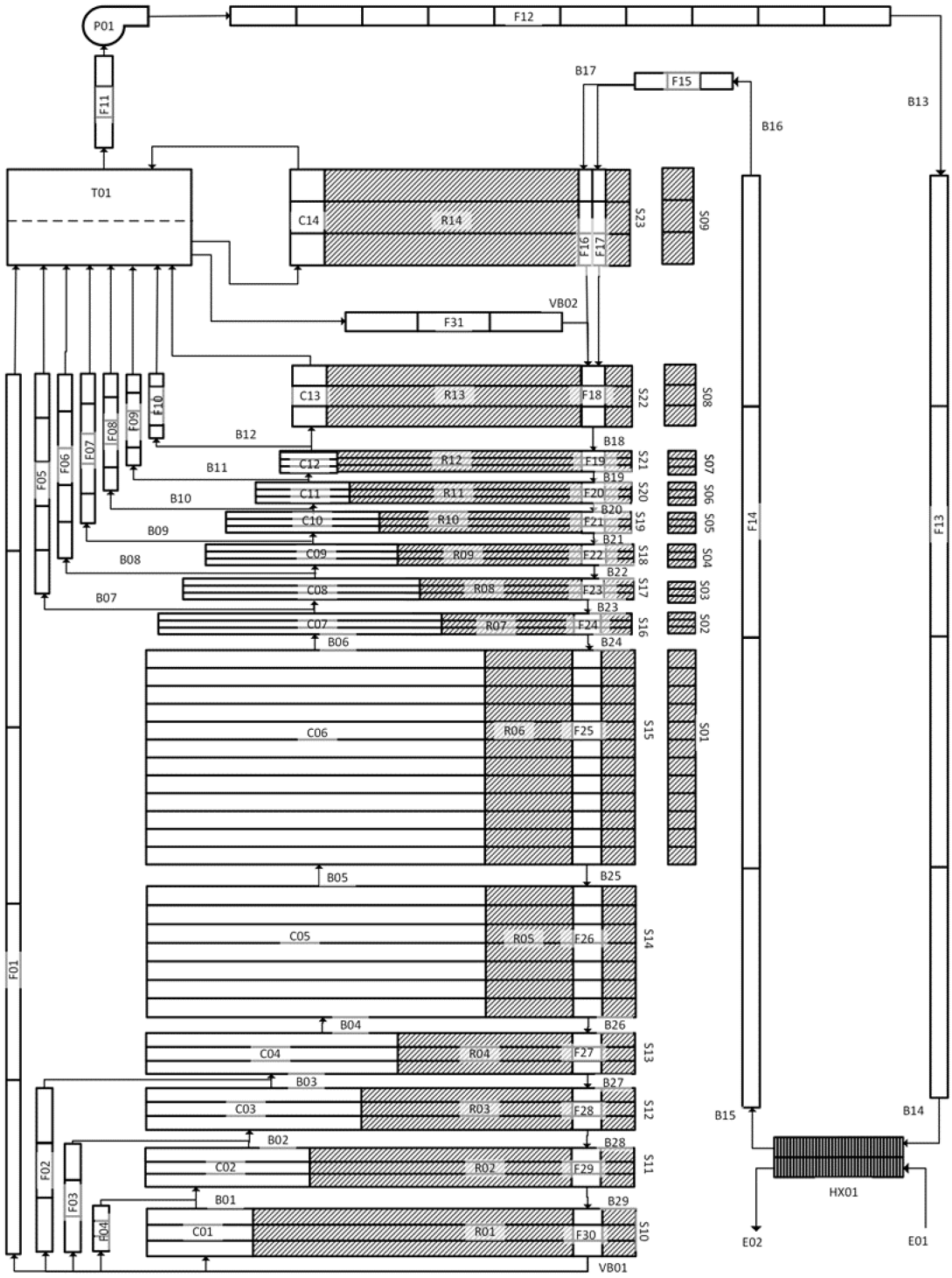

APPENDIX A. SAMPLE TRANSIENT RESULTS

A.1 Insertion of Excess Reactivity

Event Description

A control element with 3.02$ reactivity worth is assumed to be withdrawn completely over 100 seconds. The rate of reactivity insertion depends on a worth curve and the progression of the rod withdrawal. When the power level exceeds the trip setpoint, -16.8$ of reactivity is inserted to the core over 10 seconds according to an element worth curve. After 10 seconds, this reactivity is maintained, simulating the total assumed element worth. The assumptions made are summarized as below and initial conditions are provided in Table A1-1.

Power trip setpoint = 120%

Upper plenum temperature trip setpoint = 958.1K (665°C + 3%)

Power trip delay time = 2s

Temperature trip delay time = 2s

Element insertion delay after trip = 2s

Time to fully insert rods after trip = 10s

Element worth = 16.8$

Primary salt pump halving time = 2s

Intermediate velocity halving time = 1s

KP-SAM analysis results

The transient is initiated at 0 seconds with the start of reactivity insertion. Prior to a reactor trip, this positive reactivity insertion is counteracted in part by negative Doppler, moderator, and coolant feedback respectively in order of magnitude. Soon after reactor trip is initiated, the total change in reactivity of the system becomes negative and remains so despite the continuation of the reactivity insertion, as shown in Figure A1-1.

When the reactor trip is initiated, the PSP is tripped as well, causing a decrease in flow rate throughout the system. This has notable impacts on heat transfer throughout the system during the entire simulation, as this will characterizes flow behavior in the core during earlier stages of the transient and facilitate the transition to natural circulation in the long term.

KP-SAM Conclusions

A reactivity insertion of 3.02$ over 100 seconds was assumed to simulate an uncontrolled control element withdrawal. The reactor is tripped by a high flux protection signal (120%) at 9 seconds after the

© 2024 Kairos Power LLC

event initiation. Figure A1-2 shows key predicted temperatures relative to the temperature used in the MHA analysis. The temperature rises in the TRISO and fuel matrix were observed, with very little change in the Flibe temperature. The resulting temperatures, with the exception of reflector temperatures, are within the acceptance level, with significant margins. The short deviation (i.e., on the order of a few minutes) of the reflector temperature slightly above the MHA temperature is acceptable due to the time-at-temperature nature of diffusion of tritium out of graphite grains.

Fuel Performance Analysis

The power and temperature profiles were used as inputs to KP-BISON. The transient is modeled at the end of a normal operation phase that provides the adequate state of the TRISO fuel particles (e.g., failure fractions, fission product distribution, fission gas inventory, etc.).

The normal operation phase is modeled using the irradiation conditions shown in Table A1-2.

Table A1-2 shows the failure probabilities calculated by KP-BISON within the Monte Carlo calculation scheme for the TRISO failure modes for normal operation and reactivity insertion event. The results in Table A1-2 indicate that the temperature during normal operation and transient is not high enough to challenge the TRISO fuel with overpressure or Pd attack. Furthermore, Table A1-3 shows that the reactivity insertion event does not lead to any significant incremental failure.

© 2024 Kairos Power LLC

Table A1-1: Initial conditions for Insertion of Excess Reactivity Assumed Bounding Event

Parameter	Initial Condition	Rationale
Reactor initial power	102%	Assumed power measurement uncertainty
Coolant average temperature	Nominal + 3%°C	Controller deadband and measurement uncertainties
System pressure	Nominal	The effect of the system pressure is insignificant
Power distribution	Axial + radial power distribution for peaking factor Both fresh core, and equilibrium core are considered as limiting conditions	Most limiting power distribution is considered

© 2024 Kairos Power LLC

Table A1-2: 95% Confidence Level Upper Limit on In-Service Failure Fractions for Normal Operation and Reactivity Insertion Postulated Event

Failure Probability	Normal Operation	Normal Operation + Reactivity Insertion
Probability of IPyC cracking	9.75×10^{-1}	9.75×10^{-1}
Probability of SiC failure	2.26×10^{-3}	2.26×10^{-3}
Contribution due to palladium penetration	3.00×10^{-6}	3.00×10^{-6}
Contribution due to IPyC cracking	2.26×10^{-3}	2.26×10^{-3}
Probability of TRISO failure	3.00×10^{-6}	3.00×10^{-6}

© 2024 Kairos Power LLC

Table A1-3: Compromised Fractions for Normal Operation and Reactivity Insertion Postulated Event

Release Fraction	Normal Operation	Normal Operation + Reactivity Insertion
Intact	$2.25x10^{-2}$	$2.25x10^{-2}$
Compromised IPyC	$9.65x10^{-1}$	$9.65x10^{-1}$
Compromised IPyC +SiC	$2.24x10^{-3}$	$2.24x10^{-3}$
Compromised SiC	$1.03x10^{-4}$	$1.03x10^{-4}$
Compromised OPyC	$1.00x10^{-2}$	$1.00x10^{-2}$
Compromised IPyC + SiC + OPyC	$5.30x10^{-5}$	$5.30x10^{-5}$

© 2024 Kairos Power LLC

Figure A1-1: Reactivity Insertion and Reactivity Feedback After Full Rod Withdrawal

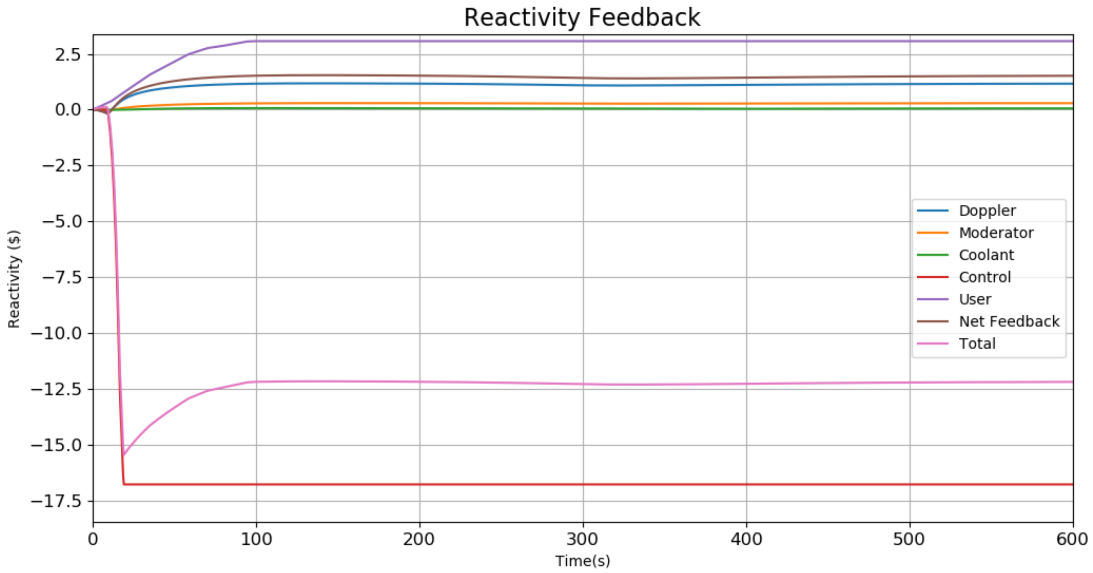

Figure A1-2: Figures of Merit During and After Reactivity Insertion

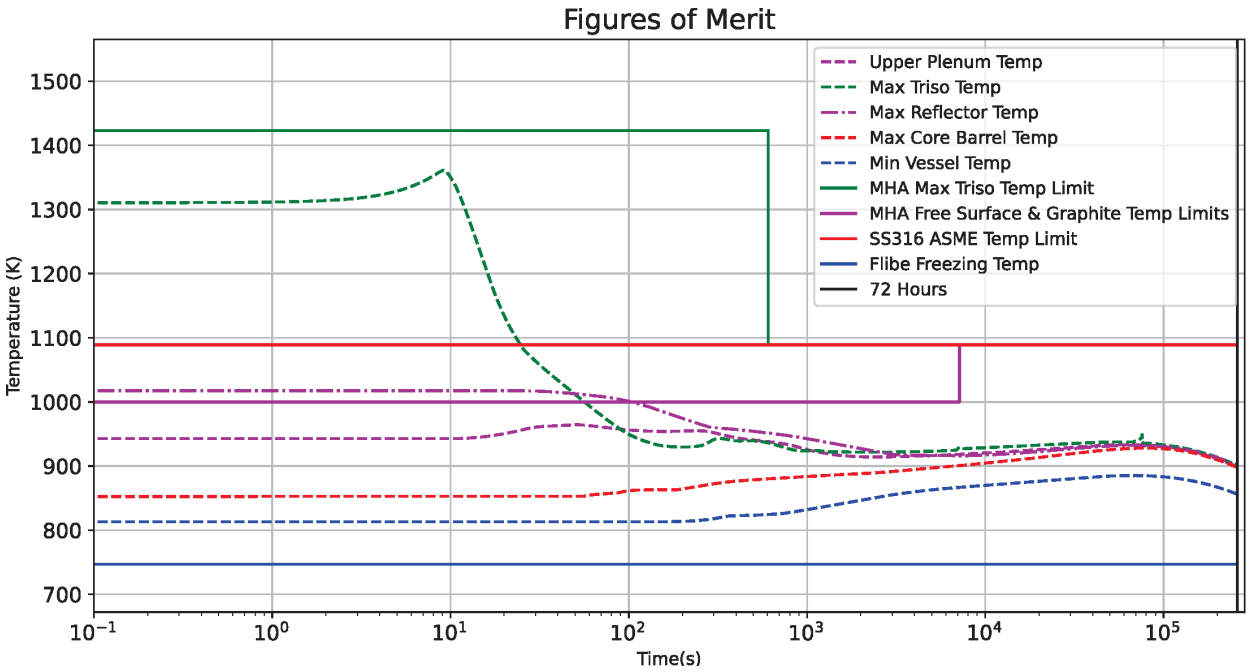

A.2 Increase in Heat Removal

Event Description

An increase in heat removal may insert positive reactivity into the system. In order to demonstrate that this event is bounded by reactivity insertions coming from the RCSS, a conservative prompt jump reactivity insertion is used to approximate the effects of an increase in heat removal.

Inherent sources of reactivity feedback in the system include the Doppler (coming from the fuel), moderator (non-fuel portions of pebbles), reflector and coolant. Since any increase in reactivity (and power) from an increase in heat removal first occurs due to the reduction in coolant temperature it is conservative to assume that both the fuel and moderator feedback only acts to resist this change. Thus, it is conservative to neglect the reactivity feedback associated with fuel and moderator heating. As a result, the only two components of reactivity feedback that need to be considered are coolant and reflector feedback. The reflector feedback is delayed relative to other feedback mechanisms but can in some states insert positive reactivity into the system as it cools down. Thus, an extra layer of conservatism is added by prescribing that the reflector and coolant both experience the same simultaneous reduction in temperature from the increase in heat removal. Additionally, yet another layer of conservatism is applied by assuming that both the coolant and reflector feedback coefficients are at their most negative across temperature ranges considered. A summary of the parameters used to drive the prompt jump approximation are provided below:

- Delayed neutron fraction = 6.08768E-3
- Coolant reactivity feedback coefficient = -1.95 pcm/°C
- Reflector reactivity feedback coefficient = -1.25 pcm/°C

The prompt jump approximation for normalized reactor power after a step insertion of reactivity is provided in the equation below where α is a reactivity feedback coefficient, β is the delayed neutron fraction and ΔT is the impose instantaneous reduction in coolant and reflector temperature.

$$P_{norm} = \frac{\beta(1 - \alpha\Delta T)}{\beta - \alpha\Delta T}$$

Analysis Results

Figure A2-1 shows the result of applying the equation above to a range of instantaneous reflector and coolant temperature reductions. In Figure A2-1 it is shown that both the reflector and the coolant would need to be reduced instantaneously by ~40°C in order to approach the overpower seen from the control rod withdrawal. Such a large global reduction in core temperature would require a massive and sustained increase in heat removal. Considering the conservatisms of neglecting moderator and Doppler feedback, the impossibility of instantaneously reducing the temperature of the core's entire Flibe and reflector volume to such an extent that it would cause an overpower like what could occur in a rod withdrawal event, and the reality that the symptoms of excessive heat removal are easily detectable; reactivity insertions originating from the RCSS bound those caused by an increase in heat removal.

© 2024 Kairos Power LLC

Figure A2-1: Normalized Reactor Power vs Instantaneous Average Fuel and Cooling Temperature Drop

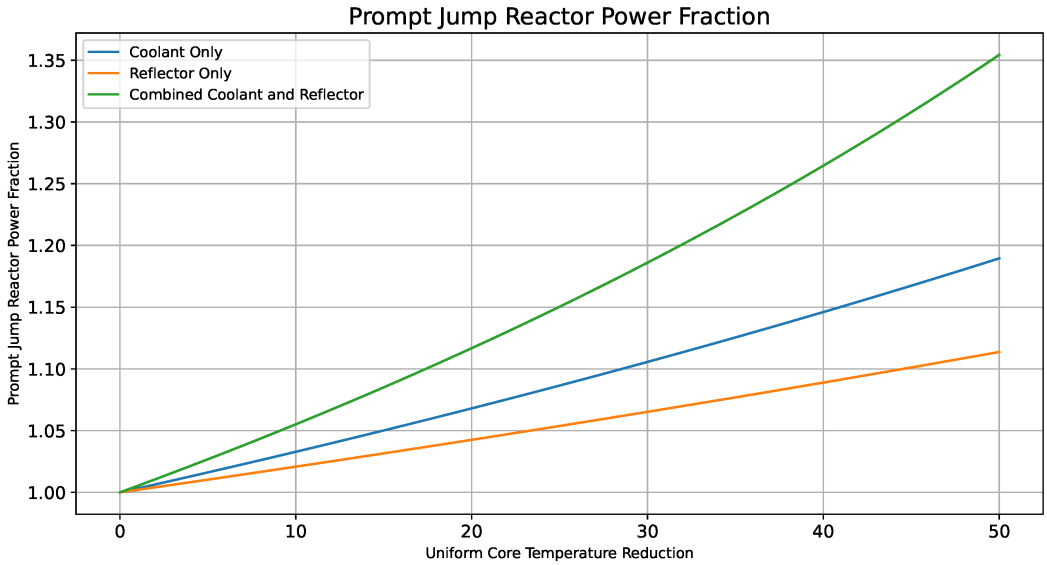

A.3 Salt Spill

Event Description

The event is described in Sections 3.2.2 and 4.5 with Tables A3-1 and A3-2 providing key input parameters and the properties of Flibe and air based on the spilled Flibe temperature and building air temperature.

When the large pipe break event occurs, the liquid through the hot leg is driven by the PSP to discharge at a high velocity. The Flibe in the cold leg, however, is expected to drain under gravity at a low velocity out of the break. The difference in the speeds affects aerosol generation rates because a higher velocity jet produces smaller size particles and thus converts a larger fraction of the discharged liquid mass into aerosols. It is assumed that both the Flibe jets through the hot and cold legs are discharged at the same pump-driven velocity and produce identical fractional amount of aerosol.

Liquid Flibe driven by the PSP is accelerated when the break occurs because of sudden decrease of the downstream pressure. The flow velocity increases until it reaches the run-off velocity at which the pump head is reduced to zero. Therefore, the run-off velocity of PSP can be considered as a bounding velocity for the velocity of Flibe out of the break. However, the run-off velocity is specific to a particular pump rotational speed. When the break occurs, not only the flow velocity but also the pump speed increases. The flow velocity at the pump outlet requires a detailed pump dynamic model. To avoid the complexity associated with the dynamic pump model, the run-off velocity is used. For this approach, the flow velocity is evaluated with the Bernoulli equation based on normal operation pump head and gravity head between the pump outlet.

Analysis Results

Aerosol generation rate due to single phase jet breakup and spilling is evaluated based on the methodology in section 4.5. Table A3-3 lists calculated values based on parameters provided in Tables A3-1 and A3-2. Using the values provided in Table A3-3, the total cumulative aerosol mass produced during the postulated double ended guillotine PHTS pipe break event is the sum of the mass through single-phase and two-phase flow:

$$m_a = m_{a,1p} + m_{a,2p} = 0.0685\ kg$$

When large amounts of Flibe is spilled from the primary system, it is expected to spread on the floor and, when the spreading ends, forms a Flibe pool. The release lasts until the temperature on the top surface drops to the Flibe melting point and a solid crust starts to form. Once the crust is formed, the evaporation process is limited by diffusion through the crust and expected to be negligible. Therefore, a key variable for the evaporative release from a Flibe pool is the top surface temperature history before it drops to the Flibe melting point.

The temperature of a Flibe pool is strongly dependent on the spreading area and depth. The reactor cell design is assumed to have a flat floor area of more than 200 m^2. However, the spreading area of the Flibe may be less than the flat floor area due to several factors:

© 2024 Kairos Power LLC

- The spreading of Flibe may be limited by the area of drip catch pan if used. The area of the drip pan would be smaller than the flat floor area.
- The spreading of Flibe may be incomplete (without covering the entire area of the reactor cell or drip pan) because of freezing at the bottom and formation of crust on the spreading front.
- Flibe may flow and accumulate at certain lower area in the reactor cell if the reactor cell in reality has a slope.

Conclusions:

Material at risk is released through four paths: evaporation from the vessel and spilled Flibe, tritium degassing and desorption, mechanical aerosolization, and oxidation of exposed structure graphite and pebbles for the pipe break event. Conservative assumptions were used in the analysis above to evaluate doses and demonstrate that the pipe break event is bounded by the MHA in terms of dose consequences.

© 2024 Kairos Power LLC

Table A3-1: Key Input Parameters

Parameters	Value
Delay time to trigger the reactor trip and PSP trip signals (seconds)	10
PSP coast down half-flow time (seconds)	2
PSP normal operation volumetric flow (m^3/s)	0.177
PSP normal operation pump head (Pa)	1.5E5
Flibe volume inside hot leg (m^3)	1.23
Flibe volume inside cold legs (m^3)	1.13
Flibe volume in the pump bowl from normal operation level to pump suction (m^3)	0.33
Break diameter (m)	0.254
Elevation difference between the break and pump outlet (m)	-10
Height of the break center line relative to the floor (m)	1
Spilled Flibe temperature (°C)	650
Building air temperature (°C)	100
Building air pressure (Pa)	1E5

© 2024 Kairos Power LLC

Table A3-2: Properties of Spilled Flibe and Building Air

Properties	Value
Density of Flibe, ρ_f (kg/m^3)	1960
Dynamic Viscosity of Flibe, μ_f (Pa s)	6.781E-3
Surface Tension of Flibe, σ_f (N/m)	0.185
Density of Air in Building, ρ_g (kg/m^3)	0.378

© 2024 Kairos Power LLC

Table A3-3: Calculated Values for the Salt Spill Event

Calculated Parameter	Value
Volume of liquid pumped out by PSP before coast down, V_{coast} (m^3)	2.28
Volume of spilled Flibe, V_{spill} (m^3)	2.69
Mass of spilled Flibe, m_{spill} (kg)	5272
Flow velocity, v_{jet} (m/s)	18.7
Sauter Mean Diameter (m)	3.63E-3
Fraction of aerosolization through jet breakup, $f_{a,jet}$	1.234E-5
Fraction of aerosolization through spilling and splashing, $f_{a,spill}$	5.89E-7
Cumulative mass of aerosols generated by single-phase jet, $m_{a,1p}$ (kg)	0.0682
Cumulative mass of aerosols generated through two-phase flow, $m_{a,2p}$ (kg)	3.64E-4

© 2024 Kairos Power LLC

A.4 Loss of Forced Circulation

Event Description

The purpose of this event is to determine if the reactor is adequately designed for long term heat up events. As such, one of the key assumptions is that only 75% of DHRS capacity is available. The loss of forced circulation overheating bounding event applied to the plant model is initiated by manually tripping the pump and reducing the head to zero nearly instantaneously. The complete loss of flow defines the beginning of the transient and occurs concurrently with a loss of intermediate coolant flow. Intermediate coolant flow is not likely to be lost during a loss of forced circulation event but is imposed in this analysis to demonstrate that intermediate coolant flow is not needed to protect the plant during a loss of forced circulation event. During this transient, it is expected that the large reduction in coolant flow through the core region results in a significant rise in temperature across the core. The rise in temperature eventually causes the reactor to trip, leading to a long-term cooling transient and the safe shutdown condition of the reactor. Initial conditions for the overheating loss of forced circulation assumed bounding event are provided in Table A4-1. A set of assumptions key to this analysis are listed in Table A4-4.

The loss of forced circulation transient was run over the course of 72 hours of simulation time. During the transient, the upper plenum temperature exceeds the trip setpoint after 23 seconds, with rod insertion following a trip delay. Prior to the rod insertion, power is reduced by reactivity feedback as the core heats up, afterwards the strong insertion of negative reactivity from the rod insertion brings the reactor power down to decay heat levels. Figure A4-1 shows key predicted temperatures relative to the temperature used in the MHA analysis.

The compromised fractions for the six states are obtained from the defect and in-service failure fractions in Table 4-3 (see Section 4.2) and Table A4-5. These are shown in Table A4-6, assuming the upper specification or bounding values.

Loss of Forced Circulation Overheating

A loss of forced circulation transient biased for overheating was performed using KP-SAM. In this simulation, it was demonstrated that decay heat removal through the DHRS can compensate for the loss of the intermediate salt flow to achieve stable cooling after the fast stage of the transient.

The TRISO temperature profile is bounded by the MHA curve, which demonstrates that the diffusional release of radionuclides from fuel is bounded by the MHA. The Flibe-cover gas interfacial temperature profile is bounded by the MHA curve, which demonstrates that the release from Flibe through evaporation is also bounded by the MHA.

The graphite reflector and fuel pebble temperature profiles are bounded by the MHA curves, which demonstrates that the tritium release is bounded by the MHA. It is shown that temperatures stay below those defined by the MHA except for the upper plenum and reflector/graphite temperatures. The MHA release analysis is conservative. The MHA margin is maintained since deviations are minimal and of short duration (as scaled relative to the corresponding X/Q window associated with the deviation) due to the conservative evaporative boundary conditions in the MHA (i.e., aggressive temperature gradients driving natural circulation) and times associated with those temperatures corresponding in the MHA

© 2024 Kairos Power LLC

(i.e., evaporation and diffusion are time-at-temperature release mechanisms). Freezing does not occur in this event and that the vessel remains below the defined temperature limit.

The power and temperature profiles were used as inputs to KP-BISON. The transient is modeled at the end of a normal operation phase that provides the adequate state of the TRISO fuel particles (e.g., failure fractions, fission product distribution, fission gas inventory, etc.). The normal operation phase is modeled using the irradiation conditions shown in Table A4-3.

The failure probabilities associated with the potential failure modes listed in Section 4.2 were obtained by a Monte Carlo simulation of 106 samples. Note: the sample size was chosen to optimize computing time. From the Monte Carlo simulation results, upper limits on the failure probabilities associated with each failure modes are obtained at a 95% confidence level using the Copper-Pearson exact method. These limits are reported in Table A4-5 for the normal operation and loss of forced circulation postulated event.

The results in Table A4-5 indicate that the temperatures during normal operation and the transient are not high enough to challenge the TRISO fuel with overpressure or Pd attack. In particular, the upper limit on TRISO failure by overpressure is only a few percent (6%) of the as-manufactured exposed kernel fraction of 5.0×10^{-5}. Furthermore, Table A4-5 shows that the TRISO fuel is more likely to fail during normal operation and that the loss of forced circulation event does not lead to any significant incremental failure. Because of the conservative assumptions used to set up the low- and high-temperature trajectories, the calculated failure probabilities are also conservative and represent upper limits for expected failure probabilities.

Loss of Forced Circulation Overcooling

While the overheating version of this event is designed to challenge the margin to maximum temperatures, the overcooling scenario is designed to challenge the margin to minimum temperatures. In this case the limiting minimum temperature is taken as the point at which Flibe freezes. In order to conservatively preclude freezing, the minimum vessel inner surface temperature is taken as a bounding surrogate for the minimum Flibe temperature. The event is initiated by manually initiating a control rod insertion, primary pump trip and intermediate flow trip at t = 0. The primary pump and intermediate flow are allowed to coast down normally. Additionally, the DHRS is modeled at 100% capacity. Initial conditions for the loss of forced circulation overcooling event are provided in Table A4-2. A set of key assumptions for the example calculation is provided in Table A4-4.

The example calculation of a cooldown biased loss of forced circulation transient was run over the course of 72 hours of simulation time. Figure A4-2 shows key predicted temperatures relative to the temperature used in the MHA analysis. Temperatures predicted by the KP-SAM model are below the temperatures defined by the MHA and freezing does not occur within 72 hours.

© 2024 Kairos Power LLC

Table A4-1: Initial Conditions for Loss of Forced Circulation Overheating Assumed Bounding Event

Parameter	Initial Condition	Rationale
Reactor initial power	102%	Assumed power measurement uncertainty
Coolant average temperature	Nominal + 3%°C	Controller deadband and measurement uncertainties
System pressure	Nominal	The effect of the system pressure is insignificant
Power distribution	Axial + radial power distribution for peaking factor Both fresh core, and equilibrium core are considered as limiting conditions	Most limiting power distribution is considered
DHRS capacity	75%	Assume one DHRS train is out of operation
Heat structure heat capacity	75%	Account for any uncertainty related to the heat capacity of solid materials in the model
Flibe heat capacity	95%	Account for uncertainty in the heat capacity of Flibe
Reactivity coefficient magnitude	75%	Reduced to conservatively bias the impact of reactivity feedback prior to reactor trip

© 2024 Kairos Power LLC

Table A4-2: Initial Conditions for Loss of Forced Circulation Overcooling Assumed Bounding Event

Parameter	Initial Condition	Rationale
Reactor initial power	98%	Assumed power measurement uncertainty Minimized stored energy
Coolant average temperature	Nominal - 3%°C	Controller deadband and measurement uncertainties
System pressure	Nominal	The effect of the system pressure is insignificant
Power distribution	Axial + radial power distribution for peaking factor Both fresh core, and equilibrium core are considered as limiting conditions	Most limiting power distribution is considered
DHRS capacity	100%	Full capacity of DHRS
Heat structure heat capacity	75%	Account for any uncertainty related to the heat capacity of solid materials in the model Minimizes stored energy and accelerates cooldown
Flibe heat capacity	95%	Account for uncertainty in the heat capacity of Flibe Minimizes stored energy and accelerates cooldown
Reactivity coefficient magnitude	Nominal	Reactor trip initiated immediately following event initiation

© 2024 Kairos Power LLC

Table A4-3: Irradiation Conditions for Simulated Normal Operation

Parameter	Value
Irradiation length (EFPD)	300
Power density (fission/m^3 s	5.7 x 10^{19}
Burnup (%FIMA)	6.0
Fast flux (n/m^2 s, E > 0.1 MeV)	7.7 x 10^{17}
Fast fluence (n/m^2 s, E > 0.1 MeV)	2.0 x 10^{25}

© 2024 Kairos Power LLC

Table A4-4: Inputs for Loss of Forced Circulation Postulated Events

Loss of Forced Circulation – Overheating		Loss of Forced Circulation - Overcooling	
Parameter	Value	Parameter	Value
Temperature trip delay time (s)	2	Time to fully insert rods after trip (s)	10
Element insertion delay after trip (s)	2		
Time to fully insert rods after trip (s)	10	Trip delay after event initiation (μs)	20
Trip worth ($ of reactivity)	16.8	Trip worth ($ of reactivity)	16.8
Primary salt pump halving time (pump seizure approximation) (s)	0.01	Primary salt pump halving time (s)	2
Intermediate velocity halving time (s)	1	Intermediate velocity halving time (s)	1
DHRS capacity (%)	75	DHRS capacity (%)	100

© 2024 Kairos Power LLC

Table A4-5: 95% Confidence Level Upper Limits on In-Service Failure Fractions for Normal Operation and Loss of Forced Circulation Postulated Events

Failure Probability	Normal Operation	Normal Operation + Loss of Forced Circulation
IPyC Cracking	9.75×10^{-1}	9.75×10^{-1}
SiC Failure	2.26×10^{-3}	2.26×10^{-3}
Contribution due to palladium penetration	3.00×10^{-6}	3.00×10^{-6}
Contribution due to IpyC cracking	2.26×10^{-3}	2.26×10^{-3}
TRISO Failure	3.00×10^{-6}	3.00×10^{-6}

© 2024 Kairos Power LLC

Table A4-6: Compromised Fractions for Normal Operation and Loss of Forced Circulation Postulated Event

Release Fraction	Normal Operation	Normal Operation + Loss of Forced Circulation
Intact	2.25×10^{-2}	2.25×10^{-2}
Compromised IPyC	9.65×10^{-1}	9.65×10^{-1}
Compromised IPyC + SiC	2.24×10^{-3}	2.24×10^{-3}
Compromised SiC	1.03×10^{-4}	1.03×10^{-4}
Compromised OPyC	1.00×10^{-2}	1.00×10^{-2}
Compromised IPyC + SiC + OPyC	5.30×10^{-5}	5.30×10^{-5}

© 2024 Kairos Power LLC

Figure A4-1: Figures of Merit – Overheating

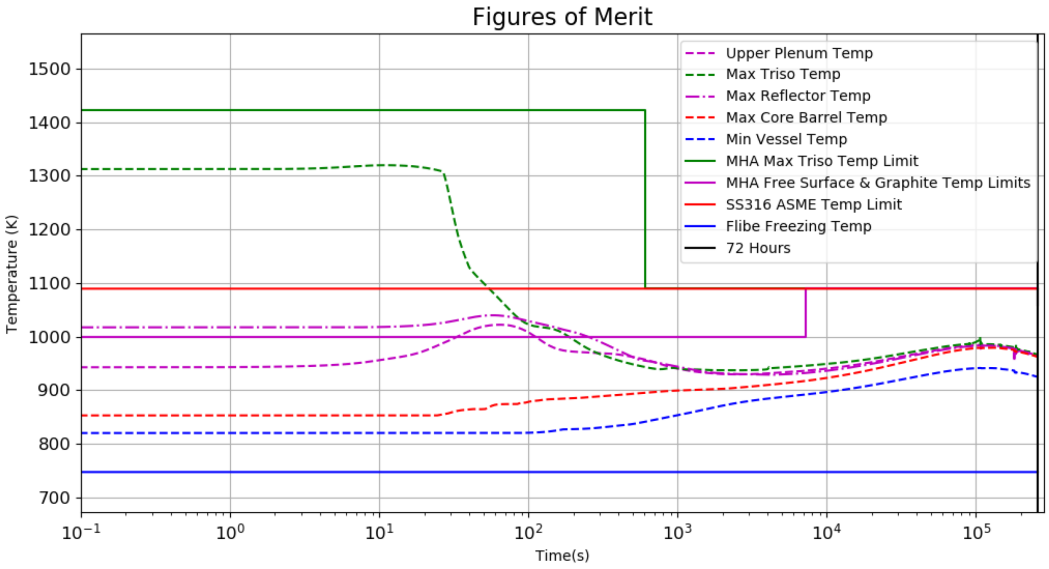

Figure A4-2: Figures of Merit – Overcooling

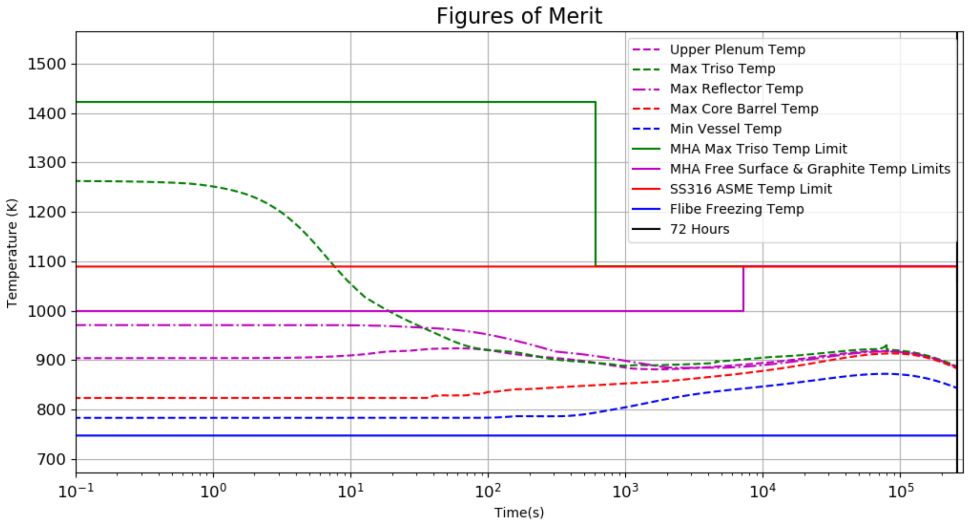

A.5 Pebble Handling and Storage System Malfunction Event

Event Description:

The PHSS break event is described in Section 3.2.2 and Section 4.5. It is caused by a hypothetical double-ended break in the pipe in the off-head conveyance system that transfers pebbles from the pebble extraction mechanism to the pebble processing/inspection system. The sequence of events includes:

- The break leads to a pebble spill from the transfer line on the floor of the PHSS hot cell.
- The isolation valve between the PHSS and the vessel is conservatively assumed to open. The break in the transferring line thus creates a path for the gas in the PHSS and vessel to leak into the PHSS hot cell.
- The reactor protection system detects the break and triggers a reactor trip signal. RCSS elements are inserted into the core to shut down the reactor.
- The decay heat is removed by the DHRS.
- The heat up of the pebbles in the PHSS system mobilizes the Flibe accumulated on the piping.
- Air ingress into the PHSS and reactor cover gas region occurs through the break.

Event Analyzed:

Conservative input parameters are listed in Table A5-1. The initial temperature of spilled pebbles is very conservative because it is equal to the Flibe temperature in the upper plenum of the core during normal operation. The pebble temperatures in the transfer line are expected to be lower due to heat loss to the cover gas and surrounding structures when they are extracted from the core.

The decay heat generation rate of 42 W is about 2% of the normal operating power per pebble, which is equivalent to the power approximately 15 minutes after a pebble is extracted from the active core. It is also conservative since pebbles are expected to be in the non-active zone for much longer than 15 minutes before they are extracted by the pebble extraction mechanism.

The gas temperature in the PHSS hot cell is used to demonstrate the methodology. Initial pressure in the PHSS is estimated based on the design objective to keep the PHSS and reactor upper head only slightly above the atmospheric pressure. The over-pressure for this estimate is about 500 Pa.

The sliding distance of pebbles in the PHSS is used to calculate the dust accumulation in the system and is an estimate for methodology demonstration. The specific wear rate of pebbles is an assumed value representative of the upper bound of the wear rate from the test results of pebbles sliding on stainless steel plate. The pebble extraction speed is evaluated based on the core design data which concludes a total of 35,000 pebbles in the core and the average residence time of 225 days during which it experiences six passes (extractions).

Analysis Results:

In order to evaluate the release of MAR and associated dose consequence due to spilled pebble and resuspended graphite dust, the MAR hold-up in the pebble graphite matrix was evaluated first. As described in section 4.5, a bounding estimate is made assuming 100% of the MAR in defective TRISO particles is released to the graphite matrix in the pebble. MAR in the graphite matrix distributes

© 2024 Kairos Power LLC

uniformly due to the large diffusion coefficients in the matrix. The MAR activity concentration (in unit of Ci/kg-graphite) in the graphite matrix is then obtained through the inventory of MAR holdup in the graphite matrix divided by the mass of the graphite matrix. Table A5-2 lists the activities for selected elements and total activities in the graphite matrix for the highest burn-up pebble.

The mass of dust in the PHSS is determined by the product of the dust accumulation rate and the time at operation. The MAR in the dust can be evaluated based on the MAR holdup in the pebble graphite matrix, assuming the same concentration of MAR in the dust and the pebble graphite matrix, when the dust is generated. However, credit is taken for radioactive isotope decay since dust accumulation occurs over many years. Credit is also taken for the extraction of non-fuel pebbles from the core region as well. It is expected that about 35% of the pebbles in the core are graphite pebbles which do not contain MAR. The total activity for MAR in the dust after an operating time of 10 years is about 0.2 Ci.

Oxidation of a spilled pebble was also simulated with the methodology in Section 4.5 and evaluates the temperature in the pebble based on 1D conduction solution of a sphere with internal heat generation. The boundary condition of the pebble is natural convection and radiation. The simulation time was 400 s. Figure A5-1 and Figure A5-2 show graphite oxidation rate and mass loss in the pebble.

The mass loss after 400 seconds is about 3.3E-5 kg, which is about 0.077% of the mass of the graphite matrix in the pebble therefore, the release fraction of MAR is 0.077% for the spilled pebbles. From Table A5-2, the total activities of MAR held up in the graphite matrix of one pebble is 20.15 Ci. The activity of MAR released through pebble oxidation of 30 pebbles was determined as 0.47 Ci, through the release fraction and the activity in the graphite matrix.

Figure A5-3 shows the temperature on the outer surface of the pebble. After 400 seconds, the temperature at the outer surface is less than 400°C which is generally considered the temperature below which the graphite oxidation rate is insignificant. The temperature in the deeper region of the pebble is higher than the temperature on the outer surface because of decay heat and oxidation heat generation. However, Figure A5-1 shows that the oxidation rate is very small after 400 seconds, indicating even the temperatures in deeper region of the pebble are low enough for oxidation termination. The results indicate the pebble is coolable within 400 seconds.

The fraction of the dust particles that are resuspended as aerosols during a PHSS line break is a function of gas velocity in the location where the dust is deposited. For conservatism, the dust particles are assumed to accumulate in the pebble transfer line and are adjacent to the break location. The dust particles in these locations, even if they are resuspended, are subject to depositing mechanisms such as inertial impact and turbulent deposition that remove them from the gas space along the path to the break location.

Resuspension fraction of graphite dust particles is evaluated with the methodology in section 4.5. The fraction depends on the gas velocity in the transfer line which is on the other hand depends on the ratio of the break area and the cross-sectional area of the pebble transfer line. The gas velocity in the pebble transfer line is close to 28 m/s for the area ratio of 1, which represents the double-ended break condition. Once the gas velocity is determined, the critical liftoff diameter of dust particles can be evaluated. The critical liftoff diameter is larger than 50 μm for area ratio less than 0.2, indicating the sizes of resuspended particles are too large to be considered as aerosols. The mass fraction is zero for area ratio less than 0.2 as expected. However, it increases rapidly for larger break area. It becomes

© 2024 Kairos Power LLC

97.9% for the double-ended break condition. This indicates that the release fraction of the dust particles in PHSS is almost 100% for a large break. From Table A5-2, the total activities in the dust in PHSS are about 0.2 Ci for an assumed 10 years of operation. For the resuspension fraction of 97.9%, the activities released due to resuspension are 0.196 Ci.

Materials at risk are released through three paths, i.e., dust resuspension, oxidation of spilled pebbles and exposed pebbles inside PHSS, and evaporations from the Flibe pool in the vessel through the break, for PHSS break event. Doses are evaluated to demonstrate that the PHSS break event is bounded by the MHA in terms of event consequences. The approach to evaluate dose consequences of PHSS break event utilize the gas space transport methodology for design basis accidents in Reference 3.

Key assumptions of the dose consequence analysis are summarized below:

- Ar-41 that is held up in closed graphite pores is conservatively released in a “puff” at time zero.
- Releases from dust resuspension and spilled pebble oxidation occur at time zero for conservatism.
- High volatility noble metals and dissolved gases in the Flibe are conservatively puff released at time zero.
- Flibe pool in the vessel has a void fraction of 1% which is considered as a bounding estimate of gas entrained by RCP during normal operation. Aerosol generation due to bubble bursting when RCP trips is considered through a conservative aerosol generation efficiency. The aerosols generated through bubble bursting are conservatively released in a “puff” at time zero.

The radiological consequences from this event are less than the MHA because:

- In-vessel postulated event evaporative releases are much lower than the MHA due to less severe in-vessel evaporative conditions applied to the postulated event analysis such as an overall shorter cumulative time at high cover-gas/Flibe interfacial temperatures and less severe natural circulation mass transfer conditions.
- The tritium releases rates, even given aggressive tritium releases from oxidized graphite, will be lower than the MHA because the in-core graphite will have significantly lower spatial temperature distributions of in core pebble carbon matrix and graphite reflector temperatures.
- Fuel releases will be reduced in the postulated event analysis because the overall initial TRISO inventories were inflated due to a hypothetically assumed un-diffused TRISO initial conditions in the MHA. As a result, lower postulated event initial conditions coupled with reduced time-at-temperatures as a driving force to diffuse those inventories out of the fuel will result in lower fuel releases.

<u>Conclusions:</u>

These conservatisms in the MHA, when taken together, provide enough dose margin to accommodate the additional release of oxidized graphite MAR and dust resuspension modeled in the proceeding sections and bound the releases of MAR for the PHSS break event.

© 2024 Kairos Power LLC

Table A5-1: Key Input Parameters for Pebble Handling and Storage System Malfunction Event

Input Parameter	Value
Fraction of defective TRISO particles in a pebble	0.0022
Number of spilled pebbles	30
Mass of graphite matrix in a pebble (kg)	0.0583
Mass of pebble (kg)	0.0428
Initial temperature of spilled pebbles (K)	923
Decay heat per pebble (W)	42
Gas temperature in the PHSS hot cell (K)	373
Initial pressure in PHSS (Pa)	1.018×10^{5}
Diameter of pebble transfer line (m)	0.254
Sliding distance of pebbles in PHSS (m)	10
Specific wear rate (μg/N m)	15
Pebble extraction speed (s^{-1})	0.0108
Geometric mean diameter of graphite dust particles (μm)	10
Geometric standard deviation of graphite dust particles	1.5
Pebble radius (m)	0.02
Pebble average density (kg/m^3)	1740
TRISO particle packing fraction (fuel region of pebble) (%)	36.8
Average TRISO particle density (kg/m^3)	3000
Graphite dust accumulation rate (kg/s)	9.27×10^{-10}

© 2024 Kairos Power LLC

Table A5-2: Total Activities and Activities for Selected Elements in Graphite Matrix in Pebbles with Highest Burnup

Element	Activity (Ci)	Activity Concentration (Ci/kg-graphite)
Cs	0.890	20.78
I	1.256	29.33
Sr	1.162	27.14
Te	0.887	20.72
Total	20.15	470.6

© 2024 Kairos Power LLC

Figure A5-1: Graphite Oxidation Rate

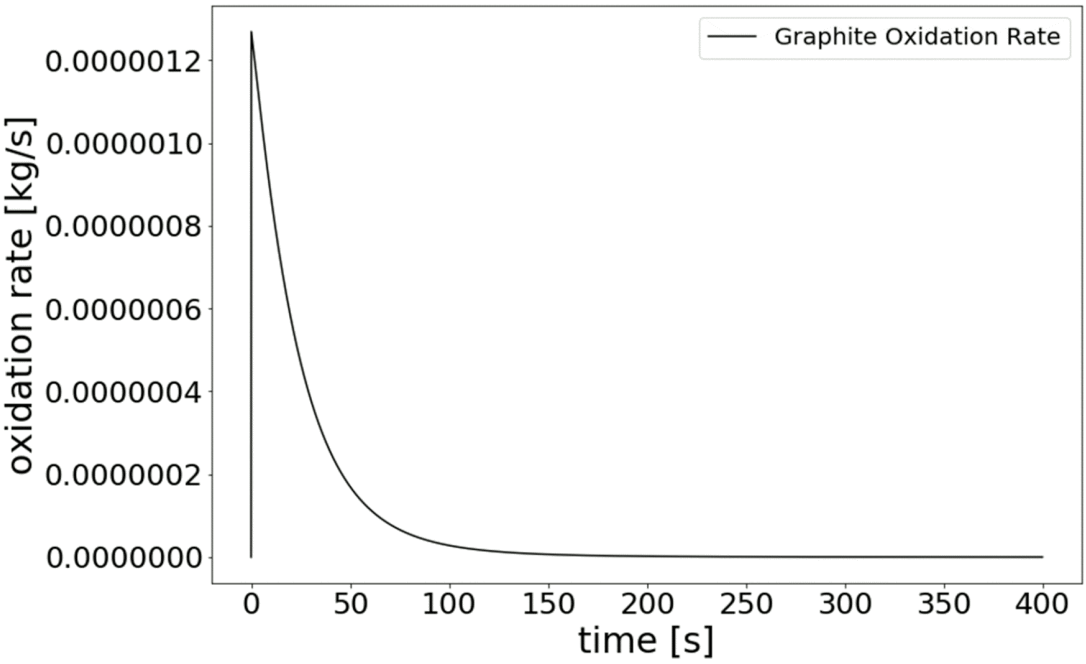

Figure A5-2: Mass Loss of Graphite Matrix and Release Fraction of MAR

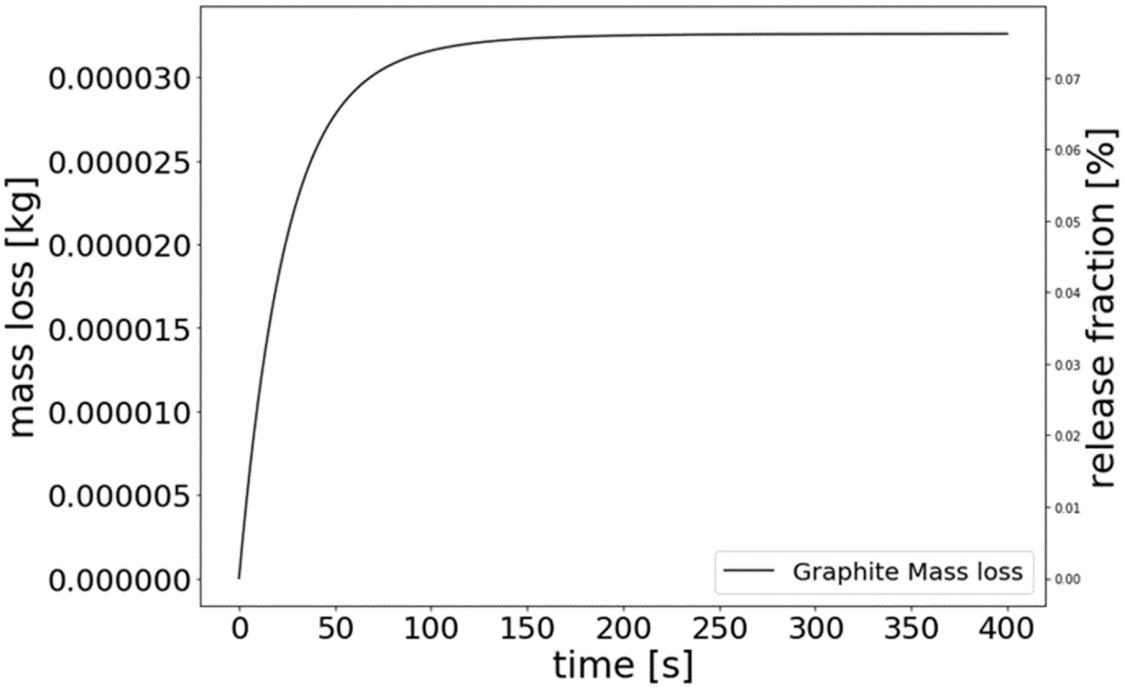
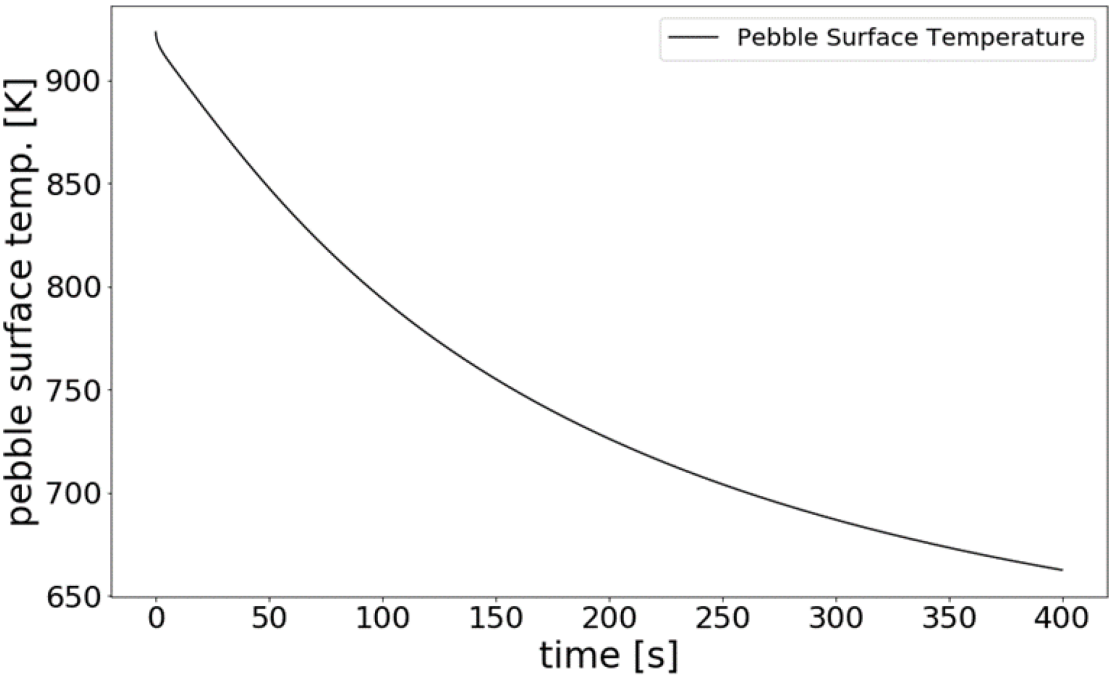
Figure A5-3: Temperature of the Outer Surface of the Pebble